Loss of a plant receptor kinase recruits beneficial rhizosphere-associated *Pseudomonas*

Authors: Yi Song[1,2], Andrew J. Wilson[1], Xue-Cheng Zhang[3,4,5], David Thoms[1,2], Reza Sohrabi[6], Siyu Song[1], Quentin Geissmann[1,2], Yang Liu[1], Lauren Walgren[1], Sheng Yang He[6,7,8] and Cara H. Haney[1,2*]

Affiliations:

[1]Department of Microbiology and Immunology, The University of British Columbia, Vancouver, Canada V6T 1Z3

[2]Michael Smith Laboratories, The University of British Columbia, Vancouver, Canada V6T 1Z4

[3]Department of Molecular Biology, Massachusetts General Hospital, Boston, MA 02114, USA

[4]Department of Genetics, Harvard Medical School, Boston, MA 02115, USA

[5]Current address: DermBiont, Inc, Boston, MA, 02111, USA

[6]Department of Energy Plant Research Laboratory, Michigan State University, East Lansing, MI, USA

[7]Department of Biology, Duke University, Durham, NC, 27708, USA

[8]Howard Hughes Medical Institute, Duke University, Durham, NC, 27708, USA

*Correspondence to: cara.haney@msl.ubc.ca

Abstract

Maintaining microbiome structure is critical for the health of both plants[1] and animals[2]. In plants, enrichment of beneficial bacteria is associated with advantageous outcomes including protection from biotic and abiotic stress[3,4]. However, the genetic and molecular mechanisms by which plants enrich for specific beneficial microbes without general dysbiosis have remained elusive. Here we show that through regulation of NADPH oxidase, *FERONIA* kinase negatively regulates beneficial *Pseudomonas fluorescens* in the *Arabidopsis* rhizosphere microbiome. By rescreening a collection of *Arabidopsis* mutants that affect root immunity under gnotobiotic conditions, followed by microbiome sequencing in natural soil, we identified a *FERONIA* mutant (*fer-8*) with a rhizosphere microbiome enriched in *P. fluorescens* without phylum-level dysbiosis. Using microbiome transplant experiments, we found that the *fer-8* microbiome was beneficial and promoted plant growth. The effect of *FER* on rhizosphere Pseudomonads was independent of its immune coreceptor function, role in development, and jasmonic acid autoimmunity. We found that the *fer-8* mutant has reduced basal levels of reactive oxygen species (ROS) in roots and that mutants deficient in NADPH oxidase showed elevated rhizosphere Pseudomonad levels. Overexpression of the *ROP2* gene (encoding a client of FER and positive regulator of NADPH oxidase[5]) in *fer-8* plants suppressed Pseudomonad overgrowth. This work shows that *FER*-mediated ROS production regulates levels of beneficial Pseudomonads in the rhizosphere microbiome.

41 **Main text**

42 Eukaryotes are associated with communities of symbiotic microorganisms (the microbiome)
43 that affect host heath and fitness[6]. In plants, the root-associated (rhizosphere) microbiome
44 affects plant growth[7], nutrient acquisition[8] and resistance to both biotic and abiotic stresses[9-11].
45 While dysbiotic microbiomes have been associated with disease in both plants[1] and animals[2],
46 in plants, enrichment of specific microbial taxa has been associated with growth promotion and
47 pathogen protection. For instance, disease outbreaks can induce the assembly of beneficial
48 microbes in the rhizosphere to enhance resistance to future disease[12,13]. Similarly, artificial
49 enrichment of beneficial taxa in the lab or in the field can promote growth and protect plants
50 from biotic and abiotic stresses[4,7,14]. These observations suggest that plants may be able to
51 regulate the abundance of a few beneficial taxa to maximize fitness. However, the genetic
52 regulators and mechanisms used by plants to control the abundance of beneficial microbes are
53 largely unknown.

54

55 *Pseudomonas fluorescens* includes well-studied plant growth-promoting (PGP) and biocontrol
56 strains[15,16]. Interestingly, *P. fluorescens* and related species are routinely enriched in
57 agricultural disease suppressive soils. For example, disease suppressive soils that confer
58 resistance to *Rhizoctonia solani*[13], wheat take all disease[17], *Fusarium* wilt[18] and black root rot[19]
59 have all been associated with the enrichment of fluorescent Pseudomonads in the soil. The
60 recurring observation that enrichment of Pseudomonads is associated with pathogen protection
61 suggests that plants may possess a mechanism to specifically recruit beneficial *Pseudomonas*
62 spp.[20-22]. In addition, certain natural accessions of *Arabidopsis thaliana* support different levels

of rhizosphere *Pseudomonas* spp. while maintaining overall highly similar microbiome compositions[23], indicating plants may have genetic mechanisms to regulate levels of beneficial *Pseudomonas* spp.

***HSM13*/*FERONIA* inhibits rhizosphere *Pseudomonas* growth**

To identify plant genes that regulate beneficial *Pseudomonas* spp. levels in the rhizosphere, We made use of 16 *hsm* (*hormone mediated suppression of MAMP triggered immunity*) mutants identified from a previous genetic screen[24]. The *hsm* mutations affect root immunity, and thus provide a genetic toolkit to identify novel genes that shape the rhizosphere microbiome. We screened these 16 *hsm* mutants[24] for their ability to support growth of the beneficial *P. fluorescens* strain WCS365 expressing the luciferase operon (*P. fluorescens* WCS365-Luc) using a 48-well plate gnotobiotic system (Extended Data Fig. 1)[23]. We found that the *hsm13* mutant harbored consistently higher levels of rhizosphere *P. fluorescens* WCS365 relative to the parental line (Extended Data Fig. 2).

To test whether increased levels of *P. fluorescens* in the *hsm13* rhizosphere also occur in the presence of a complex microbial community, we grew *hsm13* in natural soil (Methods, Fig. 1a), and plated rhizosphere samples (normalized to the rhizosphere weight) on King's B media to quantify fluorescent Pseudomonads[25] (Fig. 1b). We found that the fluorescent Pseudomonads per gram of rhizosphere were enriched more than 10-fold in the rhizosphere of *hsm13* relative to wildtype plants (Fig. 1, b and c). We found that *hsm13* is stunted in both natural soil and axenic plates (Fig. 1a, Extended Data Fig. 3, a and b), and has a root hair elongation defect

(Extended Data Fig. 3, c-e). To test whether plant morphological changes affect rhizosphere Pseudomonad levels, we tested *bri1-5* (a stunted mutant unable to perceive the growth hormone brassinolide[26]; Fig. 1a), and *ark1-1* (a root hair mutant with altered microtubule dynamics[27]). We found that both the *bri1-5* and *ark1-1* mutants have similar levels of rhizosphere fluorescent Pseudomonads as wildtype plants (Fig. 1c), suggesting that developmental defects are unlikely to underlie the enrichment of fluorescent Pseudomonads in *hsm13*.

To identify the mutation that results in enriched *Pseudomonas* spp. in *hsm13,* we crossed *hsm13* to Col-0 and performed sequencing-assisted mapping by bulk segregant analysis (Methods). We identified a genomic region with a high frequency of SNPs present in the *hsm13*-like segregant population on the short-arm of chromosome 3 (Extended Data Fig. 4). We identified four non-synonymous SNPs in that region including a G1793A missense mutation in the coding sequence of *AT3G51550* (*FERONIA*, *FER*) in *hsm13* resulting in a predicted G598E amino acid substitution in the kinase domain (Fig. 1d). The previously described *fer-4* mutant shows a similar stunted morphology (Fig. 1e) and root hair developmental defects[28]. The F1s of a *fer-4*×*hsm13* cross had high *P. fluorescens* levels and small plant size similar to *hsm13* indicating that *fer-4* is allelic to *hsm13* (Fig. 1f, Extended Data Fig. 4). The F1 progeny of a Col-0×*hsm13* cross exhibited the *P. fluorescens* levels and plant size of Col-0 plants, confirming that *hsm13* is recessive (Fig. 1f, Extended Data Fig. 4). Using the gnotobiotic system, we found that *fer-4* (CS69044) had a similarly high level of WS365-Luc as the *hsm13* mutant and that *fer-5* (Salk_029056C) had a 1.95-fold increase in WCS365-Luc (Fig. 1f), which is consistent with previous data suggesting that *fer-5* is a partial loss-of-function allele[29]. Expression of *FER*

under its native promoter (p*FER:FER-GFP*[5]) in the *fer-4* mutant completely restored the normal plant morphology and rhizosphere *P. fluorescens* WCS365 growth to wildtype levels (Fig. 1e and g). Collectively our data indicate that *hsm13 (fer-8* hereafter) carries a loss of function mutation in *FER* resulting in stunting and rhizosphere Pseudomonad overgrowth.

Microbiome profiling of *fer-8*

To determine the effect of the *fer-8* mutation on the overall rhizosphere microbiome composition, we grew *fer-8* and wildtype plants in the presence of natural soil microbiota [soil was from the same site over two consecutive years, Experiment 1 (Fig. 2) and 2 (Extended Data Fig. 5)] and performed 16S rRNA-based microbiome profiling. Samples from different years were clearly separated in the pooled PCoA analysis (Extended Data Fig. 5a) suggesting that the starting soil has the highest effect on rhizosphere microbiome composition. Despite the differences in soil composition from year-to-year, a consistently distinct microbiome composition was observed in *fer-8* relative to wildtype plants revealed by unconstrained principal coordinate analysis (PCoA), and 13.9%-18.2% of the differences in samples could be explained by plant genotype (PC2) (Fig. 2a; Extended Data Fig 5b). We observed no consistent shift in phylum level relative abundance between *fer-8* and wildtype plants (Fig. 2b; Extended Data Fig. 5). The *fer-8* microbiome had lower richness (number of Operational taxonomic units, OTUs) and Shannon diversity (a metric of species richness and evenness) compared to wildtype plants (Fig. 2c; Extended Data Fig. 5c)[30]. Although several bacterial families were enriched and depleted in each experiment, only Pseudomonadaceae were enriched in both

experiments (Fig. 2d; Extended Data Fig. 5e). These data indicate that the Pseudomonadaceae are robustly enriched in the *fer-8* rhizosphere microbiome without phylum-level dysbiosis.

The genus *Pseudomonas* includes both beneficial microbes and plant pathogens[31]. This raises the question of whether *fer-8* specifically enriches beneficial *Pseudomonas* spp., or whether pathogenic *Pseudomonas* spp. are also enriched in the rhizosphere. We selected several phylogenetically diverse *Pseudomonas* strains (including both opportunistic pathogens and beneficial microbes), along with distantly related bacterial isolates, and tested whether they are enriched in the *fer-8* rhizosphere[31]. Commensal *Pseudomonas* strains included *P. putida* WCS358, *Pseudomonas* sp. CH267, *P. simiae* WCS417, *P. fluorescens* WCS365 and *Pseudomonas* sp. SY10 (identified from the natural soil used in this study). Pathogenic or opportunistic pathogens included *P. syrinage* pv. tomato (*Pst*) DC3000, *Pseudomonas* sp. N2C3[31], *P. viridiflava* CH409[32] and *P. aeruginosa* PAO1. We found that 8 of the 9 tested *Pseudomonas* strains (with the exception of commensal strain *Pseudomonas* sp. CH267) were enriched between 2- and 18-fold in the rhizosphere of *fer-8* relative to wildtype plants (Fig. 2e). All non-*Pseudomonas* strains tested, including *Burkholderia xenovorans* LB400, *B. phytofirmans* PsJN, *Herbaspirillum seropedicae* SmR1 and *Bacillus subtilis* 3610, exhibited 2-fold or lower enrichment, or were depleted, in the rhizosphere of *fer-8* (Fig. 2e). Collectively, these data suggest that the *fer-8* mutation robustly enriches most *Pseudomonas* spp.

The *fer-8* microbiome is beneficial

Enrichment of fluorescent Pseudomonads in the rhizosphere is reminiscent of disease suppressive and growth promoting soils[13,15,33]. To test whether the *fer-8* associated microbiome is beneficial, we performed microbiome transplant experiments. We grew *fer-8* and its parental line in natural soil for 4 weeks (1st generation, 2 plants per pot, Fig. 3a). The soil from *fer-8* or the parental line was then re-planted with wildtype plants. In the rhizosphere samples from the 1st generation plants, we found an enrichment of fluorescent Pseudomonads in *fer-8* relative to its parental line (Fig. 3b and d). We observed a significant growth promotion effect of 2nd generation plants grown in the presence of a *fer-8* microbiome (Fig. 3 a, c and e, Extended Data Fig. 6). Since the beneficial effects by *Pseudomonas* spp. have been shown to be dose-dependent[34], we examined whether the growth promotion effect in the 2nd generation plants correlated with the abundance of fluorescent Pseudomonads in soil. We found a significant positive correlation between the abundance of fluorescent Pseudomonads in the rhizosphere of 1st generation plants (the soil used for 2nd generation growth) and the biomass (shoot weight) of 2nd generation plants (Pearson's correlation, $r = 0.97$, $p = 0.034$, Fig. 3f). These data suggest that a single mutation in *FER* shifts the soil microbiome into one that promotes growth for the next generation of plants.

In agriculture, suppressive soils are associated with enrichment of phylogenetically diverse *Pseudomonas* spp. While plants might have mechanisms to specifically enrich for beneficial strains, another possibility is that in the presence of the rhizosphere microbiome, that enrichment of pathogenic *Pseudomonas* may not be harmful due to competition with commensals in soil. *Pseudomonas* spp. are primarily associated with diseases of above-ground

plant tissues from bacterial leaf spot to pith necrosis. However, we found that pathogenic strains *Pst* DC3000 and *Pseudomonas* sp. N2C3 robustly cause stunting when added to the roots of gnotobiotic plants (Extended Data Fig. 7 a and b). To test if these strains can cause disease in soil, pathogenic *Pst* DC3000 and *Pseudomonas* sp. N2C3 were inoculated in the rhizosphere of plants grown in natural soil. Neither strain caused disease symptoms after inoculation to a final concentration of 10^5 and 10^6 CFU/gram of soil (Extended Data Fig. 7 c and d). These data suggest that the enrichment of *Pseudomonas* pathogens may not efficiently cause disease in the presence of a natural soil community so general enrichment of rhizosphere *Pseudomonas* might not present a risk of disease.

Jasmonic Acid (JA) signaling and innate immune receptors do not affect *Pseudomonas* enrichment

To reveal transcriptional changes in the *fer-8* mutant that could explain the increase in *Pseudomonas* colonization, we performed transcriptional profiling in both shoots and roots from *fer-8* and the parental line (Supplementary Table 1). We identified 675 up-regulated genes in the shoots of *fer-8* relative to wildtype plants (Supplementary Table 2). Surprisingly, we found only 82 up-regulated genes in *fer-8* roots relative to the parental line, and there were no significantly enriched GO terms. In contrast, we found that the genes upregulated in shoots were enriched in GO terms related to defense, response to fungi, and JA signaling (Extended Data Fig. 8, Supplementary Table 3), consistent with previous reports of JA activation in the shoots of *fer-4*[28]. *fer-8* exhibited enhanced resistance to the fungal pathogen *Botrytis cinerea*, shoot-specific expression of JA responsive genes, and enhanced anthocyanin accumulation in

193 petioles (Extended Data Fig. 8). The transcriptional changes in shoots were largely limited to
194 JA signaling while expression of other hormone signaling pathways were relatively similar
195 between *fer-8* and the parental line (Extended Data Fig. 9, Supplementary Table 4). These data
196 suggest that the *fer-8* mutation results in activation of JA signaling in shoots but not in roots.
197
198 While we did not observe changes in JA signaling in the root transcriptome, we hypothesized
199 that a shoot-to-root JA-dependent signal could affect the rhizosphere microbiome. To test
200 whether JA-mediated auto-immunity in shoots affects rhizosphere *Pseudomonas* colonization
201 in *fer-8*, we constructed a double mutant with *coi1-16* (deficient in JA perception[35]) and *fer-8*
202 (*coi1-16 fer-8*). We found that the *coi1-16 fer-8* mutant suppressed the stunting phenotype of
203 *fer-8* (Extended Data Fig. 10). However, the *coi1-16 fer-8* double mutant retained enhanced
204 *Pseudomonas* growth similar to the *fer-8* single mutant (Fig. 4a). Enhanced JA in shoots might
205 antagonize salicylic acid (SA) signaling[36]. To determine if effects on SA signaling could
206 explain the enhanced levels of *P. fluorescens* in the *fer-8* mutant, we tested rhizosphere
207 *Pseudomonas* levels in the SA perception deficient mutant (*npr1-1*)[37], the SA biosynthesis
208 mutant (*sid2-1*)[38] and the SA auto-immune mutant (*snc1*)[39]. We found no significant changes
209 in rhizosphere fluorescent Pseudomonads in SA mutants (Extended Data Fig. 11). These data
210 collectively indicate that neither JA auto-immunity nor SA-JA antagonism fully explains the
211 increase in rhizosphere *Pseudomonas* colonization in the *fer-8* mutant.
212
213 FER interacts with immune receptors and facilitates the complex formation of innate immune
214 receptor complexes that include EF-TU RECEPTOR (EFR) and FLAGELLIN-SENSING 2

(FLS2) with their co-receptor BRASSINOSTEROID INSENSITIVE 1–ASSOCIATED KINASE 1 (BAK1)[40]. We reasoned that if FER regulates Pseudomonads through its immune scaffold function, then immune receptor mutants should also increase rhizosphere Pseudomonads. However, we found that *fls2*, *efr-1* and *bak1-5* mutants all have similar levels of rhizosphere fluorescent Pseudomonads as wildtype plants when grown in natural soil (Fig. 4a). A recent study found that a mutant deficient in multiple immune receptors and vesicle-trafficking (*mfec*: *min7 fls2 efr cerk1*) causes dysbiosis in the endophytic phyllosphere microbiome and decreased alpha diversity[1]. We wondered whether the *mfec* mutant would show rhizosphere enrichment of *Pseudomonas* similar to *fer-8.* Although the enrichment of Pseudomonads in the *fer-8* was reproducible in a distinct natural soil (from Michigan State, USA), we did not observe significant enrichment of Pseudomonads in the rhizosphere of *mfec* mutants (Fig. 4b). This indicates that the mechanism of rhizosphere microbiome changes in *fer-8* is distinct from the *mfec* mutant, and that innate immune perception as well as immune scaffold functions of FER are largely dispensable for the selective enrichment of Pseudomonads in *fer-8*.

FER maintains root reactive oxygen species (ROS) to control Pseudomonads

In addition to the MAMP-triggered ROS burst (inducible ROS)[40], FER also positively regulates basal ROS levels in roots through ROP2 (a small GTPase). ROP2 is a positive regulator of plasma membrane NADPH oxidases and *fer-4* and *fer-5* mutants have reduced basal ROS levels in roots[5]. We hypothesized that loss of FER might result in decreased basal ROS resulting in *Pseudomonas* overgrowth. By staining roots with the ROS-sensitive dye H2DCF-

237 DA[5], we found a significant decrease in basal ROS levels in buffer-treated *fer-8* compared to
238 the parental line (Fig. 4c and d). Importantly, roots treated with *P. fluorescens* WCS365
239 exhibited a significant reduction in root ROS levels in both *fer-8* and the parental line (Fig. 4c
240 and d), indicating that suppression of basal root-surface ROS might be crucial for *Pseudomonas*
241 fitness in the rhizosphere.
242
243 To test if altering rhizosphere ROS levels could affect *Pseudomonas* growth in the rhizosphere,
244 we tested *Respiratory Burst Oxidase Homologues* mutants (*rbohD*, *rbohF*), which are deficient
245 in the membrane-associated NADPH oxidase and dampen apoplastic ROS production[41]. We
246 found that both *rbohD* and *rbohF* have significantly elevated rhizosphere fluorescent
247 Pseudomonads in natural soil (Fig. 4e). To test if *FER* acts through NADPH oxidase to regulate
248 rhizosphere *Pseudomonas,* we overexpressed the FER interacting client *ROP2* in *fer-8*, which
249 has previously been shown to enhance ROS in a *fer-5* mutant[5]. We found that *fer-8 ROP2OX*
250 significantly increased root ROS levels relative to *fer-8* (H2DCF signal intensity) and
251 decreased the level of fluorescent Pseudomonads observed in the *fer-8* rhizosphere (Extended
252 Data Fig. 12). By plotting the average rhizosphere fluorescent Pseudomonads levels against
253 the average ROS levels (measured by H2DCF signal intensity) in different genetic backgrounds,
254 we saw a significant negative correlation ($r = -0.74$; $p = 0.035$) between ROS and Pseudomonad
255 levels (Fig. 4f). Collectively these data indicate that *ROP2*-mediated regulation of ROS is
256 required for *FER* mediated regulation of rhizosphere Pseudomonads.
257
258

Discussion

This work revealed that *FER* regulates rhizosphere *Pseudomonas* colonization through suppressing NADPH oxidase activity. We found that genetic manipulation of ROS production in plants can shape the microbiome and gate access of beneficial commensals to the rhizosphere. Although the ROS burst is a critical step of innate immune activation in plants, we found that FER-mediated regulation of rhizosphere Pseudomonads is dependent on basal ROS rather than inducible ROS triggered by MAMP perception and innate immune receptors. From an evolutionary standpoint, this could be because roots are constitutively exposed to a MAMP-rich environment and are less sensitive to MAMPs[42]. Moreover, rhizosphere microbes can suppress pattern-triggered immunity (PTI)[43] and thus plants may rely on basal ROS levels to gate rhizosphere *Pseudomonas* colonization.

It is unclear why decreased ROS in *hsm13* relatively specifically enriches *Pseudomonas* spp. as ROS is toxic to most microbes. We speculate that root surface ROS only affects a localized region close to the root surface (rhizoplane), which may be a region where beneficial *Pseudomonas* spp. are specifically enriched[23] and therefore may be more vulnerable to plant defenses than other taxa. Spatial-temporal resolution of rhizosphere communities may reveal why manipulation of root ROS effectively gates colonization by *Pseudomonas* spp.

The enrichment of *Pseudomonas* is of agricultural interest because it is frequently associated with disease suppressive and growth promoting soils. *FER* is a versatile receptor kinase that positively regulates growth and immunity, and is thus a potential target that could be hijacked

281 by pathogens. Both the fungal pathogen *Fusarium oxysporum* and nematodes secrete functional
282 RALF-like peptides to manipulate FER activity and to promote pathogenesis[44,45]. Interestingly,
283 root associated *Pseudomonas* spp. are enriched in disease suppressive soil towards either
284 *Fusarium oxysporum* or nematodes[18,46] suggesting that pathogen manipulation of *FER*
285 signaling in crops[47,48] is a possible mechanism for increased *Pseudomonas* after pathogen
286 attack. Collectively this work has the potential to guide novel breeding and microbiome
287 engineering practices in agriculture through manipulation of FER signaling.
288

Main references

1 Chen, Tao, *et al.* "A plant genetic network for preventing dysbiosis in the phyllosphere." *Nature* **580**, 653-657. (2020)

2 Levy, M., Kolodziejczyk, A. A., Thaiss, C. A. & Elinav, E. Dysbiosis and the immune system. *Nat Rev Immunol* **17**, 219-232, (2017).

3 de Vries, F. T., Griffiths, R. I., Knight, C. G., Nicolitch, O. & Williams, A. Harnessing rhizosphere microbiomes for drought-resilient crop production. *Science* **368**, 270-274, (2020).

4 Berendsen, R. L., Pieterse, C. M. & Bakker, P. A. The rhizosphere microbiome and plant health. *Trends in plant science* **17**, 478-486 (2012).

5 Duan, Q., Kita, D., Li, C., Cheung, A. Y. & Wu, H. M. FERONIA receptor-like kinase regulates RHO GTPase signaling of root hair development. *PNAS* **107**, 17821-17826, (2010).

6 Rosenberg, E. & Zilber-Rosenberg, I. Microbes Drive Evolution of Animals and Plants: the Hologenome Concept. *MBio* **7**, e01395, (2016).

7 Lugtenberg, B. & Kamilova, F. Plant-growth-promoting rhizobacteria. *Annual review of microbiology* **63**, 541-556, (2009).

8 Zhang, J. *et al. NRT1.1B* is associated with root microbiota composition and nitrogen use in field-grown rice. *Nat Biotechnol*, (2019).

9 Kwak, M. J. *et al.* Rhizosphere microbiome structure alters to enable wilt resistance in tomato. *Nat Biotechnol*, (2018).

10 Dimkpa, C., Weinand, T. & Asch, F. Plant-rhizobacteria interactions alleviate abiotic stress conditions. *Plant, cell & environment* **32**, 1682-1694, (2009).

11 Abdelaziz, M. E. *et al.* Piriformospora indica alters Na+/K+ homeostasis, antioxidant enzymes and LeNHX1 expression of greenhouse tomato grown under salt stress. *Scientia Horticulturae* **256**, (2019).

12 Berendsen, R. L. *et al.* Disease-induced assemblage of a plant-beneficial bacterial consortium. *The ISME journal* **12**, 1496-1507, (2018).

13 Mendes, R. *et al.* Deciphering the rhizosphere microbiome for disease-suppressive bacteria. *Science* **332**, 1097-1100 (2011).

14 Vurukonda, S. S., Vardharajula, S., Shrivastava, M. & Sk, Z. A. Enhancement of drought stress tolerance in crops by plant growth promoting rhizobacteria. *Microbiol Res* **184**, 13-24, (2016).

15 Haas, D. & Defago, G. Biological control of soil-borne pathogens by fluorescent Pseudomonads. *Nat Rev Microbiol* **3**, 307-319, (2005).

16 Bakker, P. A., Pieterse, C. M. & van Loon, L. C. Induced Systemic Resistance by Fluorescent *Pseudomonas* spp. *Phytopathology* **97**, 239-243, (2007).

17 Weller, D. M., Howie, W. J. & Cook, R. J. Relationship between *in vitro* inhibition of *Gaeumannomyces graminis* var. *tritici* and suppression of take-all of wheat by fluorescent Pseudomonads. *Phytopathology* **78**, 1094-1100 (1988).

18 Mazurier, S., Corberand, T., Lemanceau, P. & Raaijmakers, J. M. Phenazine antibiotics produced by fluorescent Pseudomonads contribute to natural soil suppressiveness to *Fusarium* wilt. *The ISME journal* **3**, 977 (2009).

19 Stutz, E., Défago, G. & Kern, H. Naturally Occurring Fluorescent Pseudomonads

Involved in Suppression of black root rot of tobacco. *Phytopathology* **76**, 181-185 (1986).

20 Shipton, P. Monoculture and soilborne plant pathogens. *Annual review of phytopathology* **15**, 387-407 (1977).

21 Simon, A. & Sivasithamparam, K. Pathogen-suppression: a case study in biological suppression of *Gaeumannomyces graminis* var. *tritici* in soil. *Soil Biology and Biochemistry* **21**, 331-337 (1989).

22 Cook, R. J. The influence of rotation crops on take-all decline phenomenon. *Phytopathology* **71**, 189-192 (1981).

23 Haney, C. H., Samuel, B. S., Bush, J. & Ausubel, F. M. Associations with rhizosphere bacteria can confer an adaptive advantage to plants. *Nature plants* **1**, (2015).

24 Zhang, X. C., Millet, Y. A., Cheng, Z., Bush, J. & Ausubel, F. M. Jasmonate signalling in *Arabidopsis* involves SGT1b-HSP70-HSP90 chaperone complexes. *Nature plants* **1**, (2015).

25 Johnsen, K. & Nielsen, P. Diversity of *Pseudomonas* strains isolated with King's B and Gould's S1 agar determined by repetitive extragenic palindromic-polymerase chain reaction, 16S rDNA sequencing and Fourier transform infrared spectroscopy characterisation. *FEMS microbiology letters* **173**, 155-162, (1999).

26 Noguchi, T. *et al.* Brassinosteroid-insensitive dwarf mutants of *Arabidopsis* accumulate brassinosteroids. *Plant Physiol* **121**, 743-752, (1999).

27 Eng, R. C. & Wasteneys, G. O. The microtubule plus-end tracking protein ARMADILLO-REPEAT KINESIN1 promotes microtubule catastrophe in *Arabidopsis*. *Plant Cell* **26**, 3372-3386, (2014).

28 Guo, H. *et al.* FERONIA Receptor Kinase Contributes to Plant Immunity by Suppressing Jasmonic Acid Signaling in *Arabidopsis thaliana*. *Curr Biol* **28**, 3316-3324 e3316, (2018).

29 Haruta, M., Sabat, G., Stecker, K., Minkoff, B. B. & Sussman, M. R. A peptide hormone and its receptor protein kinase regulate plant cell expansion. *Science* **343**, 408-411, (2014).

30 Kim, B. R. *et al.* Deciphering Diversity Indices for a Better Understanding of Microbial Communities. *J Microbiol Biotechnol* **27**, 2089-2093, (2017).

31 Melnyk, R. A., Hossain, S. S. & Haney, C. H. Convergent gain and loss of genomic islands drive lifestyle changes in plant-associated *Pseudomonas*. *The ISME journal* **13**, 1575-1588, (2019).

32 Haney, C. H. *et al.* Rhizosphere-associated *Pseudomonas* induce systemic resistance to herbivores at the cost of susceptibility to bacterial pathogens. *Mol Ecol* **27**, 1833-1847, (2018).

33 Carrion, V. J. *et al.* Pathogen-induced activation of disease-suppressive functions in the endophytic root microbiome. *Science* **366**, 606-612, (2019).

34 Raaijmakers, J. M. *et al.* Dose-response relationships in biological control of *Fusarium* wilt of radish by *Pseudomonas* spp. *Phytopathology* **85**, 1075-1080 (1995).

35 Ellis, C. & Turner, J. G. A conditionally fertile *coi1* allele indicates cross-talk between plant hormone signalling pathways in *Arabidopsis thaliana* seeds and young seedlings. *Planta* **215**, 549-556, (2002).

36 Spoel, S. H. *et al.* NPR1 modulates cross-talk between salicylate- and jasmonate-dependent defense pathways through a novel function in the cytosol. *Plant Cell* **15**, 760-770, (2003).

37 Cao, H., Bowling, S. A., Gordon, A. S. & Dong, X. Characterization of an *Arabidopsis* Mutant That Is Nonresponsive to Inducers of Systemic Acquired Resistance. *Plant Cell* **6**, 1583-1592, (1994).

38 Dewdney, J. *et al.* Three unique mutants of *Arabidopsis* identify *eds* loci required for limiting growth of a biotrophic fungal pathogen. *The Plant journal* **24**, 205-218, (2000).

39 Zhang, Y., Goritschnig, S., Dong, X. & Li, X. A gain-of-function mutation in a plant disease resistance gene leads to constitutive activation of downstream signal transduction pathways in *suppressor of npr1-1, constitutive 1*. *Plant Cell* **15**, 2636-2646, (2003).

40 Stegmann, M. *et al.* The receptor kinase FER is a RALF-regulated scaffold controlling plant immune signaling. *Science* **355**, 287-289, (2017).

41 Miller, G. *et al.* The plant NADPH oxidase RBOHD mediates rapid systemic signaling in response to diverse stimuli. *Science signaling* **2**, ra45, (2009).

42 Zhou, F. *et al.* Co-incidence of Damage and Microbial Patterns Controls Localized Immune Responses in Roots. *Cell* **180**, 440-453 e418, (2020).

43 Yu, K. *et al.* Rhizosphere-Associated *Pseudomonas* Suppress Local Root Immune Responses by Gluconic Acid-Mediated Lowering of Environmental pH. *Curr Biol* **29**, 3913-3920 e3914, (2019).

44 Masachis, S. *et al.* A fungal pathogen secretes plant alkalinizing peptides to increase infection. *Nat Microbiol* **1**, 16043, (2016).

45 Zhang, Xin, *et al*. Nematode-encoded RALF peptide mimics facilitate parasitism of plants through the FERONIA receptor kinase. *Molecular Plant* **13**, 1434-1454, (2020).

46 Hussain, M. *et al.* Bacterial community assemblages in the rhizosphere soil, root endosphere and cyst of soybean cyst nematode-suppressive soil challenged with nematodes. *FEMS microbiology ecology* **94**, (2018).

47 Zhang, X., Yang, Z., Wu, D. & Yu, F. RALF–FERONIA Signaling: Linking Plant Immune Response with Cell Growth. *Plant Communications* **1**, (2020).

48 Campbell, L. & Turner, S. R. A Comprehensive Analysis of RALF Proteins in Green Plants Suggests There Are Two Distinct Functional Groups. *Frontiers in Plant Science* **8**, (2017).

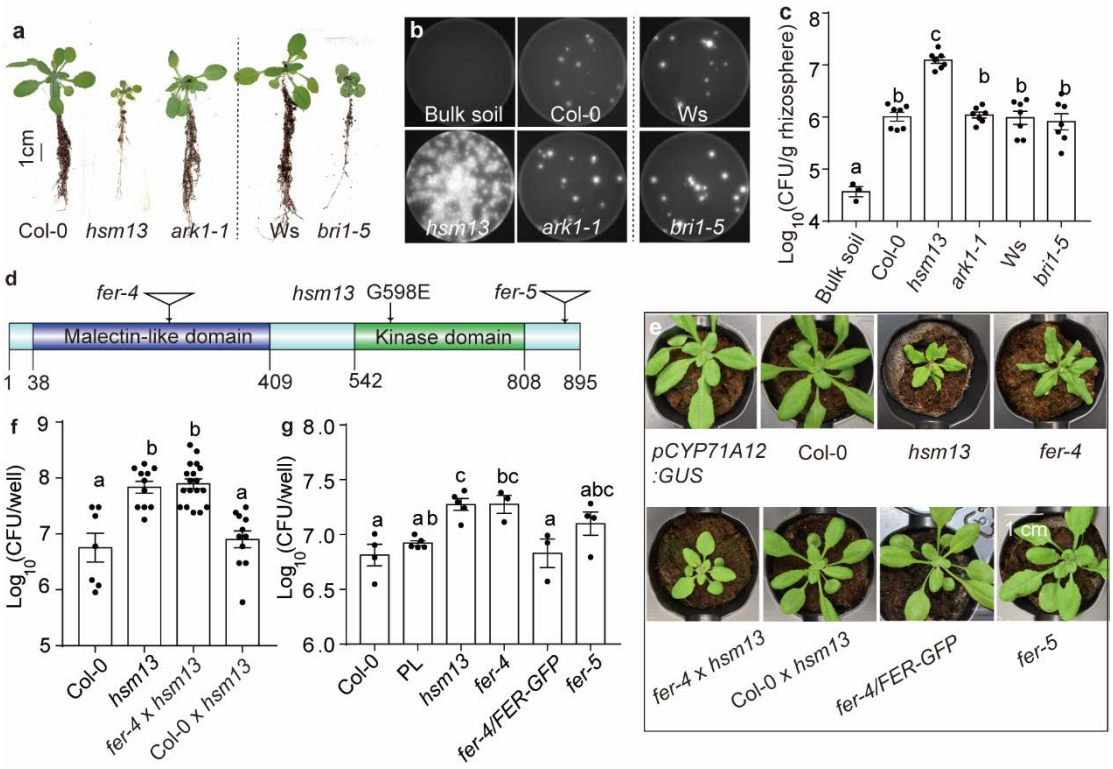

Fig. 1. *hsm13/fer-8* harbors a high level of rhizosphere Pseudomonads due to a missense mutation in the *FERONIA* receptor kinase.

(**a**) Morphology of wildtype plants (Col-0 and Ws ecotypes), and mutants *hsm13*, *ark1-1* (Col-0 background), and *bri1-5* (Ws background) when grown in natural soil; (**b**) *hsm13* harbored a high level of root-associated fluorescent Pseudomonads when grown in natural soil, while other mutants with similar developmental defects do not affect rhizosphere fluorescent Pseudomonads levels. Rhizosphere samples were plated on King's B and imaged under UV light. **(c)** Quantification of fluorescent colonies per gram of rhizosphere samples. n=3-7. **(d)** The FER protein domains and the insertion/mutation positions of alleles described in this study. **(e)** Phenotypes of 3-week-old wildtype plants (Col-0), parental line (PL; *pCYP71A12:GUS*), *hsm13, fer-4*, *fer-5*, F1 crosses (*fer-4*×*hsm13* or Col-0×*hsm13*) and *fer-4/FER-GFP*. **(f)** F1 crosses between *fer-4*×*hsm13* have high level of rhizosphere Pseudomonads relative to Col-0, while Col-0×*hsm13* F1s restored Pseudomonads levels similar to wildtype plants. n=7, 11, 17 and 11 from left to right. **(g)** *fer-4 and fer-5* mutants have elevated levels of Pseudomonads in a hydroponic seedling assay. Each point represents the average of >6 plants from a single experiment. ANOVA and Turkey's HSD were used for **c**, **f**, and (**g**) to determine significance; different letters indicate $p < 0.05$. Mean ± SEM is shown.

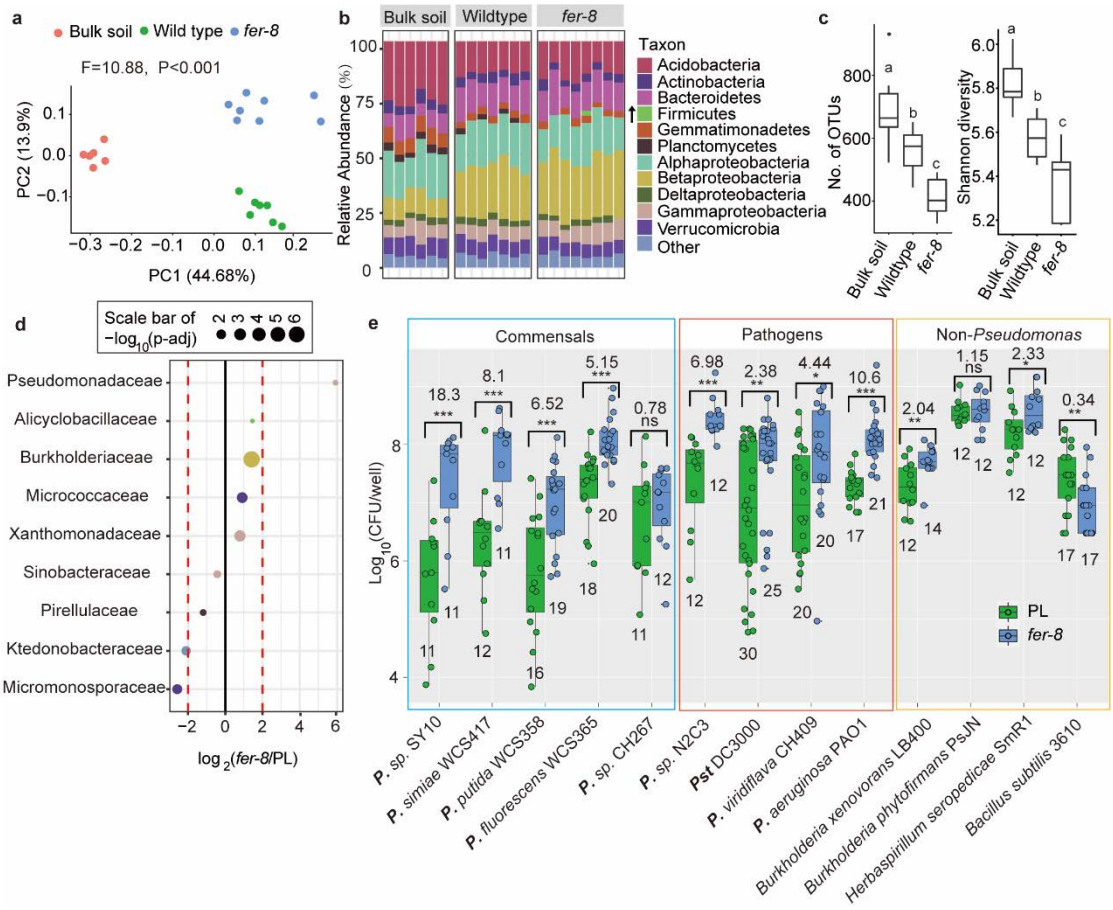

Fig. 2. Pseudomonadaceae are enriched in the rhizosphere microbiome of *fer-8*. **(a)** Principal coordinate analysis (PCoA, based on the relative abundance of OTUs) of bulk soil and rhizosphere samples of *fer-8* and wildtype (Col-0) from Experiment 1. n=6-8. **(b)** Relative abundance of bacterial phyla or classes (for Proteobacteria) in bulk soil and rhizosphere samples. The arrow shows that only Firmicutes were significantly enriched in the rhizosphere of *fer-8* relative to the parental line (PL; 3.53-fold, calculated by DESEQ2). **(c)** Number of OTUs and Shannon diversity indexes in the bulk soil and rhizosphere samples. ANOVA and Turkey's HSD were used to determine statistical significance, $p < 0.05$. **(d)** Significantly differentially abundant families between *fer-8* and wildtype. Colors show the taxonomic information for each family, and the dot size indicates the -$\log_{10}$ transformed adjusted p value for taxa with p<0.1. **(e)** Quantification of individual bacterial strains grown in the rhizosphere of *fer-8* and the PL under gnotobiotic conditions. Student's t test was used to compare the significance between *fer-8* and PL for each strain (*p<0.05, **p<0.01, ***p<0.001). Boxplots (with median and first and third quartiles) and each data point are shown. Numbers denote the number of biological replicates over 2-3 independent experiments.

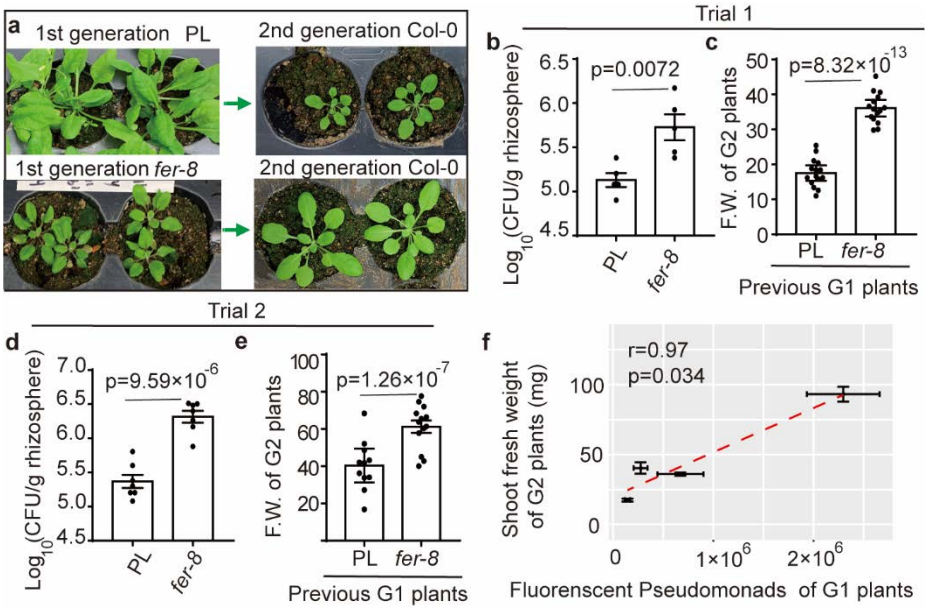

Fig. 3. The *fer-8* rhizosphere microbiome confers growth promotion to the next generation of plants.

(a) Representative images of the parental line (PL) and *fer-8* grown in natural soil (generation 1, G1) and wildtype Col-0 plants (generation 2, G2) are shown. **(b)** Fluorescent Pseudomonads were quantified in the rhizosphere of the parental line (PL) and *fer-8* in G1 plants after 4 weeks of growth, n=5. **(c)** The shoot fresh weight (F.W.) of G2 wildtype plants grown in the soil from microbiome transplants from the PL- or *fer-8*-cultivated soil, n=15. **(d-e)** A second replicate of the experiments shown in (**b-c)** was performed, n=7 for (**d**), n=11 and 13 for PL and *fer-8* in (**e**). Student's t tests were used to determine statistical significance in (**b-e**). **(f)** The average fluorescent CFU counts from the first generation PL and *fer-8* plants were plotted against the average shoot F.W. of the next generation of plants grown in the same soil. A linear trend line (red dashed line) and Pearson's correlation r are shown. Each data point represents the average value of all plants from one independent experiment from (**b**) to (**e**) with ±SEM.

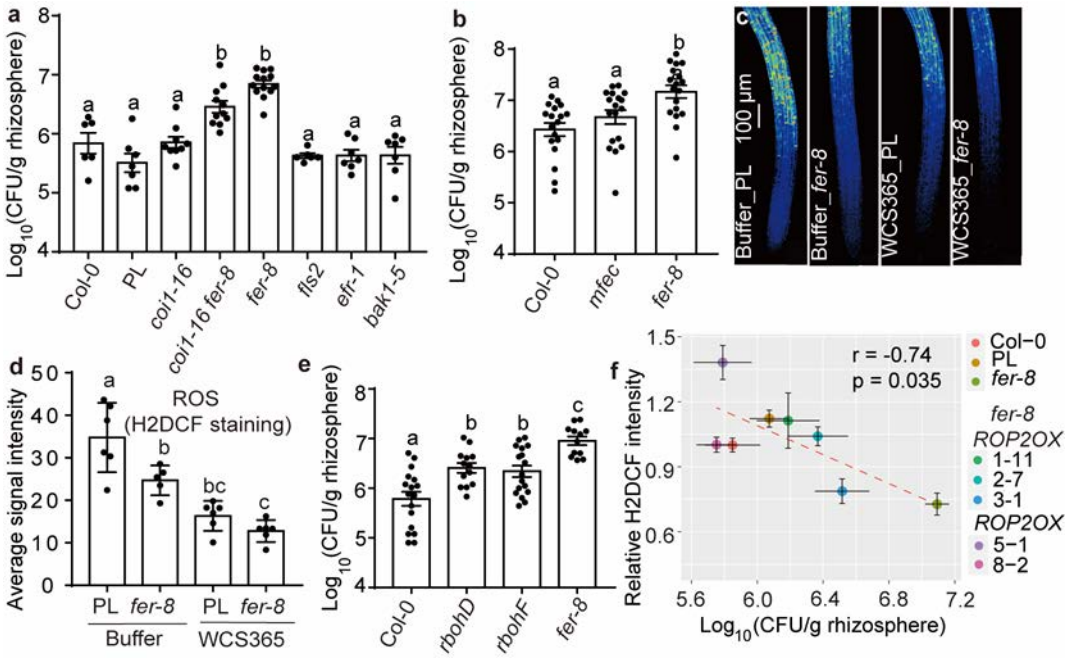

Fig. 4. Root ROS negatively regulates rhizosphere *Pseudomonas*. (a) Mutants deficient in immune receptors that are interaction partners of FER (*fls2*, *efr-1*, *bak1-5*), and the JA receptor (*coi1-16*) do not affect rhizosphere *Pseudomonas* levels, and *fer-8 coi1-16* double mutant does not restore the *fer-8 Pseudomonas* overgrowth phenotype. n = 6, 7, 9, 11, 13, 6, 7, 7 from left to right. (**b**) A quadruple mutant deficient in *min7, fls2, efr* and *cerk1* (*mfec*) does not change rhizosphere Pseudomonad level as *fer-8*. n=18 from three independent experiments. (**c**) Representative images of H2DCF-DA (ROS-binding dye) stained roots of the parental line (PL) and *fer-8* pre-treated with buffer or *P. fluorescens* WCS365. (**d**) Quantified average H2DCF-DA signal intensity in roots from two independent experiments. (**e**) Mutants deficient in NADPH oxidase (*rbohD/F*) show elevated rhizosphere fluorescent Pseudomonads when grown in soil. n=17, 13, 17 and 12 from left to right (3-4 independent experiments). (**f**) The average $\log_{10}$(fluorescent CFU/g rhizosphere) from different genotypes were plotted against the average relative H2DCF staining signaling intensity. A linear trend line (red dashed line) is shown and Pearson's correlation was used to determine significance (p=0.035). Different letters indicate $p < 0.05$ by ANOVA and Tukey's HSD in a, b, d and e.

480 **Methods**

481 **Plant materials and growth methods**

482 *Arabidopsis* seeds were surface sterilized (washed in 70% ethanol for 2 min, 10% bleach for 2
483 min, and 3 times in sterile water), and stored at 4°C for at least 2 days before use. For assays
484 on plates with solid media, seedlings were grown on 1/2× MS medium with 1% phytoagar and
485 1% sucrose. Plates were grown at 22°C under 90-100 µE light on a 12 hours light / 12 hours
486 dark cycle. The *Arabidopsis* Col-0 ecotype was used as the wildtype genetic background in this
487 work, *fls2*[49], *efr-1*[50], *bak1-5*[51], and *min7 fls2 efr cerk1* (*mfec*)[1] were reported previously. The
488 *ark1-1* mutant has a 35Spro:*EB1b*-GFP reporter, which does not alter the root hair phenotype[27].

489

490 **Gnotobiotic rhizosphere bacterial quantification assay**

491 The assay (Extended Data Fig. 1) was performed as described previously[23]. Briefly, seeds were
492 germinated on Teflon mesh disks in 300 µL MS media with 2% sucrose in 48-well plates. After
493 10 days, the media was changed to 270 µL media without sucrose (1×MS, 0.1% MES buffer)
494 so that bacteria rely on plant root exudate as a carbon source. After 2 more days, 30 µL of *P.*
495 *fluorescens* WCS365 transformed with the lux operon from *Aliivibrio fisheri* (WCS365-Luc
496 hereafter) was added. Two days after inoculation, media containing bacteria from the
497 rhizosphere in 48-well plates was transferred to opaque white 96-well plates prior to reading
498 to avoid background from the plants and Teflon mesh, and Luc photo counts were measured
499 using a Spectra Max i3 plate reader (Molecular Devices). Any plants with translucent or water-
500 soaked leaves were discarded from the assay and not used for bacterial treatment. To generate
501 WCS365-Luc, a transposon containing the *Aliivibrio fisheri* LUX operon was integrated into

the *P. fluorescens* WCS365 genome by conjugation with *Escherichia coli SM10pir* containing pUT-EM7-LUX[52]. To ensure that the insertion did not affect WCS365 growth promotion ability, we confirmed that WCS365-Luc promoted lateral root growth to a similar level as wildtype WCS365 (Extended Data Fig. 1). We found a linear relationship between the WCS365-Luc bacterial CFU counts and the Luciferase signal (Extended Data Fig. 1), indicating that the WCS365-Luc strain can be used to approximate bacterial numbers in the rhizosphere.

Mapping of *hsm13*

The (*FER*) gene was cloned by bulk segregant analysis[53]. We hypothesized that the same mutation might cause both stunting and rhizosphere *Pseudomonas* enrichment in *hsm13,* and so we used stunting to screen for *hsm13*-like segregants. Briefly, we backcrossed *hsm13* to wildtype plants (Col-0) and identified 30 stunted F2 segregates (*hsm13* like) from 140 F2 plants. We found that all F3s from these lines were stunted indicating they were homozygous for the mutation leading to stunting. We then sampled 90 plants (3 plants from each F2 line, one leaf per plant) and extracted DNA from each leaf separately. Genomic DNA samples were quantified using Quant-iT™ PicoGreen™ dsDNA Reagent (Invitrogen). DNA from different samples was mixed at equimolar ratios. A 1:1 mix of DNA from Col-0 and *pCYP71A12:GUS* (the parental line of *hsm*13) was also sequenced as a reference sample. Paired-end sequencing (150 bp reads) was performed on an Illumina HiSeq by Novogene. After filtering, approximately 35 million single-end reads (approximately 37X coverage after trimming, mapping and filtering) and 34 million single-end reads (approximately 37X coverage) were

524 mapped to the TAIR 10 *Arabidopsis* reference genome for the *hsm13* segregates population
525 and the pooled reference samples, respectively[54]. After SNP calling relative to the TAIR10
526 reference genome, 333 and 486 non-synonymous SNPs were identified in *hsm13* segregates
527 and the pooled reference samples, respectively. P_{SNP} was calculated as Mutant SNP / (Mutant
528 SNP+ wildtype SNP) in Excel. SNPs present in both *hsm13* segregates and the pooled reference
529 samples were discarded from further analysis.
530
531 **Harvesting rhizosphere samples**
532 Natural soil for the majority of experiments (except Fig. 4b) was harvested from the UBC farm
533 (49°15.0'N, 123°14.4'W), Vancouver, British Columbia, Canada. This is a disturbed site on the
534 UBC farm that was naturally colonized by wild *Arabidopsis thaliana*. The top 10-20 cm of soil
535 was collected and sieved (3-mm sieve) to remove rocks, insects and plant debris. *Arabidopsis*
536 seedlings were grown on ½ x MS plates with 1% sucrose for 8-10 days before transplanting to
537 soil. We blended additional inorganic growth materials and soils to improve drainage and plant
538 health. The final soil substrate consisted of 1:0.5:1 natural soil: calcine clay (Turface): perlite
539 for microbiome sequencing and other studies using natural soil. Both rhizosphere and bulk soil
540 samples were harvested at 17-20 days after transplanting.
541
542 The experiment to quantify fluorescent *Pseudomonas* in the rhizosphere of *hsm13* and *mfec*
543 (Fig. 4b) was performed in natural soil collected in Michigan, USA. Plants were grown in
544 "*Arabidopsis* Mix" greenhouse potting soil [equal parts of Suremix (Michigan Grower
545 Products), medium vermiculate and perlite] and was autoclaved once before use. Individual

546 pots were supplemented with natural soil slurry prepared from a soil where wild accessions of
547 *Arabidopsis* were found at Michigan State University's Southwest Michigan Research and
548 Extension Center (Benton Harbor). To prepare soil slurry, 25g of the soil was mixed with 1
549 liter of autoclaved ddH_2O for 30 min on an orbital shaker, filtered through a 70-um cell strainer
550 and 20 mL of soil slurry was supplemented to each pot uniformly by top irrigation. Plants were
551 grown under relative humidity set at 50%, temperature at 22 °C, light intensity at 100 µE m^{-2}
552 s^{-1} and photoperiod at a 12:12 hours dark: light cycle. Four-week-old plants were used
553 for rhizosphere sampling based on the protocol below.
554
555 To collect rhizosphere samples, we collected roots and closely-adhered soil. To harvest
556 rhizosphere samples, pots were inverted to transfer the soil and whole plant to a gloved hand.
557 The soil was then gently loosened from the root until just the roots and closely-adhered soil
558 remained. Gloves were cleaned with 70% ethanol between samples, and fresh gloves were used
559 between genotypes. Rhizosphere samples were weighed and buffer was added to 0.05 g/mL
560 (7.5 mM $MgSO_4$ and 20% glycerol). Samples were homogenized using a Tissuelyser (2 x 90
561 seconds at 25 rps). Samples were serially diluted and 100 µl of the bulk soil (0.0025 g/ml) or
562 rhizosphere samples (0.00025 g/mL) were plated on King's B plates and imaged using a UV
563 light source.
564
565 **Rhizosphere microbiome transplant assay**
566 For microbiome transplant experiments, we grew first-generation plants (either *fer-8* or the
567 parental line) for 3.5-4 weeks (2 plants/pot) in natural soil to allow assembly of a genotype-

specific rhizosphere microbiome. We then cut the shoots of the first-generation plants and thoroughly mixed all soil from same genotype together in a sterilized container. We then immediately (the same day) put the mixed soil (with genotype-specific microbiomes) into new clean pots to grow second-generation plants. The trays and growth chamber were sterilized with 70% ethanol before the experiment and all plants were watered with autoclaved water for both the first and second generation plants. Different genotypes were put in separate trays side by side in the same growth chamber and grown under 80-100 μE light on a 12 hour light/12 hour dark cycle. For first generation plants, about 15% of the plants were bolting 4 weeks after transplanting, we only chose non-bolting plants for the rhizosphere sampling to avoid effects of differences in developmental stage. For both generation 1 and 2 plants, 1L of 1/4x Hoagland's fertilizer was added to each tray.

16S rRNA microbiome sample preparation, sequencing and analysis.

For microbiome sequencing, four individual rhizosphere or bulk soil samples were pooled as one replicate. Sample processing and sequencing was performed as described in the Earth Microbiome Project Illumina 16S rRNA protocol (www.earthmicrobiome.org). Briefly, total soil or rhizosphere DNA was extracted using the PowerSoil® DNA Isolation kit (MoBio Laboratories, Carlsbad, CA). DNA concentrations were determined using a Quant-iT™ PicoGreen™ dsDNA Assay Kit. Paired end 300 bp sequencing was performed on an Illumina MiSeq. Adaptor sequences were trimmed with cutadapt and DADA2 was used to generate an amplicon sequence variant (ASV) table[55]. The Qiime2 implementation of vsearch was used to bin ASVs at 97% identity and the q2-feature-classifier was used to assign taxonomy using a

590 naive Bayesian approach. Principle covariate analysis was performed using Bray-Curtis
591 dissimilarity of relative abundances (OTU level) with the vegan package in R. Differentially
592 abundant families were identified using the DESEQ2 package[56].
593
594 **Transgenic plants**
595 To overexpress *ROP2*, a gene-specific primer pair was used to amplify the coding sequence of
596 *ROP2* (Forward: 5'-ATATCTAGAATGGCGTCAAGGTTTATAAAGT-3' and reverse: 5'-
597 ATACTGCAGTCACAAGAACGCGCAACGGTTC-3'), with the restriction enzyme sites for
598 *Xba*1 and *Pst*1 added to the forward and reverse primers, respectively. The PCR product was
599 digested by *Xba*1 and *Pst*1 enzymes and subcloned into a binary vector pCambia1300[57]. The
600 sequence was confirmed by Sanger sequencing, and the plasmid was introduced into
601 *Agrobacterium* GV3101 for floral dip transformation of *Arabidopsis* (Col-0 and *fer-8*). T1 and
602 T2 transformants were selected/confirmed in 1/2× MS with 1% sucrose and 50 µg/mL
603 hygromycin.
604
605 **Plant genotyping**
606 Primers for *fer-4'*are listed here[29]: P1 5'-GATTACTCTCCAACAGAGAAAATCCT-3', P2
607 5'-CGTATTGCTTTTCGATTTCCTA-3', P3 5'-ACGGTCTCAACGCTACCAAC-3', P4 5'-
608 TTTCCCGCCTTCGGTTTA-3'; and primers for Salk_029056C: LP 5'-
609 TGGTAGGATTCCGTTAAAATGC-3', RP 5'-CAGAGTATTTCAGACGGCAGC-3', LB
610 5'-ATTTTGCCGATTTCGGAAC-3'. For detection of *ROP2OX* in T1 lines, we used a pair of

611 primer targeting the *35S* promoter and *ROP2* gene (5'-CTATCCTTCGCAAGACCCTTC-3';
612 5'-GCAACGGTTCTTATTCTTTTTCT-3'), respectively.

613 For *fer-8 coi1-16* double mutant, F2 progeny of *fer-8* × *coi1-16* were selected on ½× MS
614 agar plates supplemented with 20 μM MeJA, and seedlings insensitive to JA-mediated root
615 growth inhibition were selected as *coi1-16* homozygous lines, and *fer-8* allele specific SNP
616 detection primers were designed by a web tool (http://ausubellab.mgh.harvard.edu/). The
617 primer (5'-ACATCGTCATCTTGTGTCCT
618 TGATGGG-3', 5'-GGGTTCAAGGCTGGACGAGCG-3') can specifically amplify wildtype
619 *FER* fragment but not FER^{G598E} allele (10-500 ng template DNA, elongation temperature: 57
620 degree for 25 cycles). The selected double mutants were confirmed by sanger sequencing.

621

622 **Rhizosphere growth of non-tagged commensals**

623 Rhizosphere commensals strains were grown in the rhizosphere of *fer-8* and the parental line
624 (*pCYP71A12:GUS*). All bacterial strains were cultured in LB broth or solid LB media without
625 antibiotics at 29°C. *Pseudomonas* sp. SY10 was isolated by plating a rhizosphere sample from
626 natural soil on King's B, selecting a fluorescent colony and streaking for single colonies. The
627 identity as a *Pseudomonas* sp. was determined by amplifying the 16S rRNA with primers 8F
628 (5'-AGAGTTTGATCCTGGCTCAG-3') and 1392R (5'-ACGGGCGGTGTGTRC-3'), and
629 sequencing with primer 8F. To quantify CFUs, *fer-8* or the parental line were grown as
630 described above for the gnotobiotic system and bacteria were added to a final $OD_{600} = 0.00002$
631 in 300 μl. The media containing bacteria surrounding plant roots was serially diluted and plated
632 to calculate CFUs. For most of the strains, rhizosphere samples were serially diluted and plated

633 on LB plates 2 days after inoculation, while samples of *Burkholderia phytofirmans* PsJN and
634 *Herbaspirillum seropedicae* SmR1 were plated at 4 days after inoculation. *Pst* DC3000 and *P.*
635 *viridiflava* CH409 were plated at 50-72 hours after inoculation due to slow growth in the
636 rhizosphere. Bacterial strains used in this study were previously described: *Pseudomonas* sp.
637 CH267[23], *P. fluorescens* WCS365[58], *P. simiae* WCS417[59], *P. aeruginosa* PAO1[60], *P. putida*
638 WCS358[58], *Bacillus subtilis* NCIB 3610[61], *Burkholderia xenovorans* LB400[62], *Herbaspirillum*
639 *seropedicae* SmR1[63], *Burkholderia phytofirmans* PsJN[64], *P. syringae* pv. tomato (*Pst*)
640 DC3000[65], *Pseudomonas* sp. N2C3[66,] *P. viridiflava* CH409[32]. *Pseudomonas* sp. SY10 was
641 identified in the natural soil used in this study.
642
643 **qRT-PCR.**
644 RNA was extracted using an RNAeasy isolation kit (Qiagen). RNA samples were treated with
645 Turbo DNA-free (Ambion) kit and single-stranded cDNA was generated from 1-2 µg RNA
646 using Superscript III (Invitrogen) and Oligo dT primers following the manufacturer's
647 instructions. Quantitative RT-PCR was performed on a 7,500 Fast Real-Time PCR machine
648 (Applied Biosystems) using SYBRTM Green Master Mix kit (ThermoFisher). Primers for
649 qRT-PCR are listed here[32]: *PDF1.2*, 5'- CTTATCTTCGCTGCTCTTGTTC-3' and 5'-
650 TGGGAAGACATAGTTGCATGAT-3'; *VSP1*: 5'-CTCAAGCCAAACGGATCG-3' and 5'-
651 TTCCCAACGATGTTGTACCC-3; *VSP2*, 5'-TCAGTGACCGTTGGAAGTTGTG-3' and 5'-
652 GTTCGAACCATTAGGCTTCAATATG-3'.
653
654 **RNA Sequencing and data analysis.**

For RNA sequencing, plants were grown on ½× MS with 1% phytoagar and 1% sucrose. For both the parental line (*pCYP71A12:GUS*) and *hsm13*, samples were harvested at 11 days after germination. Shoots from 2 plants or roots from 5 plants were pooled for each sample. RNA was extracted using a Qiagen RNAeasy isolation kit. RNA samples with a concentration higher than 300 ng/uL and RIN number high than 8 were used for library preparation. Construction of libraries and sequencing were performed at the Michael Smith Genome Sciences Center (http://www.bcgsc.ca/). Paired end 75 bp RNA-sequencing was performed using an Illuminia Hi-seq 2500 platform. High quality reads were mapped to the Tair 10 genome using Bowtie2[67], and transcript quantification was performed with RSEM[68]. Differential expression analysis was performed in R (https://www.R-project.org/.) with the DESeq2 package[56]. Differentially expressed genes were filtered by $p_{adj} < 0.1$. GO enrichment analysis was done by AgriGO[69]. The core JA responsive genes were those that were induced in response to JA treatment at all timepoints from 1 to 16 hours (a total of 12 sampling points)[70], and all other hormone responsive genes were obtained from a previous publication[71]. The Heatmap.2 function from gplots package in R were used to generate heatmaps.

Infection assay. *Botrytis cinerea* infection assays were performed as described[72]. Leaves 7-9 from 4-week old plants were excised and placed adaxial side down onto 1% agar plates for infection. 6 µL of 5×10^5 spores/ml was dropped onto the abaxial leaf surface. Lesion diameters were measure at 3 days after inoculation.

For *Pst* DC3000 and *Pseudomonas* sp. N2C3 inoculation in soil, six-day-old *Arabidopsis* seedlings were grown on ½× MS agar with 1% sucrose and transferred into natural soil [1:0.5:1 natural soil: calcine clay (Turface): perlite]. Inoculation was performed 1 or 2 days after transplanting. Overnight bacterial cultures were centrifuged and washed in 10 mM $MgSO_4$ three times before being diluted to an OD_{600} of 0.5 and 0.05. One milliliter of bacterial inoculum at OD_{600}=0.5 or 0.05 for each pot (approximately 70 gram soil mixture) was added to the soil taking care to not touch the seedlings to reach a final concentration of 3×10^5 and 3×10^6 CFU/gram soil, respectively. The same volume of 10 mM $MgSO_4$ was used as a buffer control. Different groups were grown side by side in the same tray, but were watered separately in different trays to avoid cross contamination.

For *Pst* DC3000 and *Pseudomonas* sp. N2C3 inoculation on plates, seeds were germinated on 1/2× MS plates (without sucrose), grown for 6 days, and inoculated with 5 µL bacteria (OD_{600}=0.05). The same volume of 10 mM $MgSO_4$ was used as a buffer control. The plates were scanned 7 days after inoculation, and the plants were weighed on the same day.

Detecting ROS in roots

ROS detection was performed using 2',7'-dichlorodihydrofluorescein diacetate (H2DCF-DA) fluorescent dye. Plants were grown on ½× MS agar plates supplemented with 1% sucrose for 4 days. Roots were inoculated with 3 µL of buffer (10 mM $MgSO_4$) or *P. fluorescens* WCS365 (OD_{600}=0.01), and seedlings were imaged 24 hours after inoculation. H2DCF-DA was dissolved in DMSO (10 mg/mL) and then diluted to a 500 mM stock (10×) in 0.1 M PB buffer

(pH 7.0) and stored at -20ºC. Before use, H2DCF-DA aliquots were thawed in the dark, stored on ice, and diluted to a 1× working concentration in 2 mL ½× MS media with 0.1% MES [2-(N-Morpholino) ethanesulfonic acid sodium salt]. Whole seedlings were transferred to a 12-well plate with 2 mL staining solution per well and stained for 15 minutes at room temperature in the dark. Imaging chambers were constructed according to a JOVE protocol[73]. Imaging chambers were molded from Poly(dimethylsiloxane) gel. A 1.5% agar pad was placed into a chamber, and roots were rinsed in ½× MS and mounted onto the pad. Glass strips placed at both ends of the glass slide provided consistent coverslip spacing and root positioning directly against the coverslip, which allowed for consistent optical resolution and fluorescence signal during image acquisition. Confocal images were acquired with a 10×/0.40 NA objective on a Leica SP8 laser scanning confocal microscope using a white light laser. H2DCF-DA was excited with a 504 nm laser and a HyD detector was used to capture emission between 511 nm – 611 nm, with detection time-gated with 0.3 – 12 ns to reduce autofluorescence. To ensure that all H2DCF-DA emitted fluorescence above the background was captured, large 3D image stacks (depth of ~120-150 microns) were taken at 2.408 µm steps (total of 50-60 images per root). Images were converted to .tiff files using FIJI[74], and root area was traced manually. The H2DCF-DA signal density was quantified based on 2D maximum intensity image projections in FIJI and the total intensity was divided by the root area.

For H2DCF signal detection in *fer-8* ROP2OX lines (Extended Data Fig. 12), four day old seedlings (grown on ½× MS agar supplemented with 1% sucrose) were stained in a H2DCF solution as described above. Seedlings were transferred onto new ½× MS agar plates for

720 imaging. A Leica M205FA fluorescence stereo microscope equipped with a Leica PLAN APO
721 2.0× CORR objective was used for high throughput imaging of two to four seedlings per image.
722 Images were acquired with a GFP filter set (excitation filter ET470/40 nm- emission filter
723 ET525/50 nm) at 2 or 5 seconds exposure time per experiment. Fluorescence signal intensity
724 along the first ~2 mm from the root tip was quantified using FUJI, and the background was
725 averaged and subtracted for each image.
726
727 **Statistics and data processing**
728 Student's t-tests (two-tailed) were used to compare the statistical significance between pairs of
729 samples. ANOVA and Turkey's HSD were used to determine the statistical significance during
730 multiple comparison using R (www.r-project.org). For CFU data, data were found to be
731 normal after log transformation. All statistics were performed on the log-transformed data.
732
733 To compare the significance of the difference of gene expression between the parental line and
734 *fer-8* (Extended data Fig. 9), we first ranked all the genes within the same sample according to
735 their absolute expression values within a single genotype. For genes from each hormone
736 pathway, we performed normal bootstrap on 5000 replicates, and calculated the mean sign of
737 differential expression of all genes within a given hormone pathway (if expression of a gene is
738 higher, same or lower in *fer-8* relative to the parental line, the sign would be 1, 0 and -1,
739 respectively). We asked whether genes from a pathway are more likely to be upregulated in
740 *fer-8* compared to the parental line relative to the mean sign of non-hormone-responsive genes.

741 P values were calculated based on the normal distribution of mean signs from 5000 bootstrap
742 dataset for each pathway.

743

744 Relative H2DCF values in Fig. 4e were calculated by normalizing raw values to the average of
745 Col-0 from the respective independent experiment.

746

747 **Methods references**

748 49 Gómez-Gómez, L. & Boller, T. FLS2: an LRR receptor-like kinase involved in the
749 perception of the bacterial elicitor flagellin in *Arabidopsis*. *Mol Cell* **5**, 1003-1011,
750 (2000).
751 50 Zipfel, C. *et al.* Perception of the bacterial PAMP EF-Tu by the receptor EFR restricts
752 *Agrobacterium*-mediated transformation. *Cell* **125**, 749-760, (2006).
753 51 Schwessinger, B. *et al.* Phosphorylation-dependent differential regulation of plant
754 growth, cell death, and innate immunity by the regulatory receptor-like kinase BAK1.
755 *PLoS genetics* **7**, e1002046 (2011).
756 52 Lane, M. C., Alteri, C. J., Smith, S. N. & Mobley, H. L. Expression of flagella is
757 coincident with uropathogenic *Escherichia coli* ascension to the upper urinary tract.
758 *PNAS* **104**, 16669-16674 (2007).
759 53 James, G. V. *et al.* User guide for mapping-by-sequencing in *Arabidopsis*. *Genome*
760 *biology* **14**, R61, (2013).
761 54 Li, H. & Durbin, R. Fast and accurate short read alignment with Burrows-Wheeler
762 transform. *Bioinformatics* **25**, 1754-1760, (2009).
763 55 Callahan, B. J. *et al.* DADA2: High-resolution sample inference from Illumina
764 amplicon data. *Nature methods* **13**, 581-583, (2016).
765 56 Love, M. I., Huber, W. & Anders, S. Moderated estimation of fold change and
766 dispersion for RNA-seq data with DESeq2. *Genome biology* **15**, 550, (2014).
767 57 Ding, Y. *et al.* Opposite Roles of Salicylic Acid Receptors NPR1 and NPR3/NPR4 in
768 Transcriptional Regulation of Plant Immunity. *Cell* **173**, 1454-1467.e1415, (2018).
769 58 Geels, F. & Schippers, B. Selection of antagonistic fluorescent *Pseudomonas* spp. and
770 their root colonization and persistence following treatment of seed potatoes. *Journal of*
771 *Phytopathology* **108**, 193-206 (1983).
772 59 Lamers, J., Schippers, B. & Geels, F. Soil-borne diseases of wheat in the Netherlands
773 and results of seed bacterization with pseudomonads against *Gaeumannomyces*
774 *graminis* var. *tritici*, associated with disease resistance. *Cereal breeding related to*
775 *integrated cereal production*, 134-139 (1988).
776 60 Holloway, B. W. Genetic recombination in *Pseudomonas aeruginosa*. *Journal of*
777 *general microbiology* **13**, 572-581, (1955).
778 61 Earl, A. M., Losick, R. & Kolter, R. *Bacillus subtilis* genome diversity. *Journal of*
779 *bacteriology* **189**, 1163-1170, (2007).

780 62 Bedard, D. L. *et al.* Rapid assay for screening and characterizing microorganisms for
781 the ability to degrade polychlorinated biphenyls. *Applied and environmental*
782 *microbiology* **51**, 761-768 (1986).
783 63 Baldani, J., Baldani, V., Seldin, L. & Döbereiner, J. Characterization of *Herbaspirillum*
784 *seropedicae* gen. nov., sp. nov., a root-associated nitrogen-fixing bacterium.
785 *International Journal of Systematic and Evolutionary Microbiology* **36**, 86-93 (1986).
786 64 Sessitsch, A., *et al. Burkholderia phytofirmans* sp. nov., a novel plant-associated
787 bacterium with plant-beneficial properties. *Int. J. Syst. Evol. Microbiol.* **55**, 1187–1192,
788 (2005).
789 65 Cuppels, D. A. Generation and Characterization of *Tn*5 Insertion Mutations in
790 *Pseudomonas syringae* pv. *tomato*. *Applied and environmental microbiology* **51**, 323-
791 327, (1986).
792 66 Price, M. N. *et al.* Deep annotation of protein function across diverse bacteria from
793 mutant phenotypes. *BioRxiv*, 072470 (2016).
794 67 Langmead, B., Trapnell, C., Pop, M. & Salzberg, S. L. Ultrafast and memory-efficient
795 alignment of short DNA sequences to the human genome. *Genome biology* **10**, R25,
796 (2009).
797 68 Li, B. & Dewey, C. N. RSEM: accurate transcript quantification from RNA-Seq data
798 with or without a reference genome. *BMC bioinformatics* **12**, 323, (2011).
799 69 Tian, T. *et al.* agriGO v2.0: a GO analysis toolkit for the agricultural community, 2017
800 update. *Nucleic acids research* **45**, W122-w129, (2017).
801 70 Hickman, R. *et al.* Architecture and Dynamics of the Jasmonic Acid Gene Regulatory
802 Network. *Plant Cell* **29**, 2086-2105, (2017).
803 71 Nemhauser, J. L., Hong, F. & Chory, J. Different plant hormones regulate similar
804 processes through largely nonoverlapping transcriptional responses. *Cell* **126**, 467-475,
805 (2006).
806 72 Genenncher, B. *et al.* Nucleoporin-Regulated MAP Kinase Signaling in Immunity to a
807 Necrotrophic Fungal Pathogen. *Plant Physiol* **172**, 1293-1305, (2016).
808 73 Kirchhelle, C. & Moore, I. A simple chamber for long-term confocal imaging of root
809 and hypocotyl development. *JoVE (Journal of Visualized Experiments)*, e55331 (2017).
810 74 Schindelin, J. *et al.* Fiji: an open-source platform for biological-image analysis. *Nature*
811 *methods* **9**, 676-682, (2012).
812

813 **Acknowledgments:**

814 We thank Fred Ausubel for critical reading of the manuscript and generously providing the
815 *hsm* mutant collection, Alice Y. Cheung, Zhiyong Wang, Xin Li, Yuelin Zhang, and Geoffrey
816 Wasteneys for kindly providing seed stocks, and Martin Hirst's lab for assistance with
817 sequencing. **Funding:** This work was supported by an NSERC Discovery Grant (NSERC-
818 RGPIN-2016-04121) and Weston Seeding Food Innovation grants awarded to C.H.H.. Y.S.

819 was supported by a kick-start award from Michael Smith Laboratories (UBC) and a fellowship
820 from the Chinese Postdoctoral Science Foundation. Early stages of this work were supported
821 by NIH R37 grant GM48707 and NSF grants MCB-0519898 and IOS-0929226 awarded to
822 Fred Ausubel.

823

824 **Author contributions:**

825 C.H.H. and Y.S. conceived of the project and designed experiments. Y.S. performed the
826 majority of experiments and data analysis. X.C.Z. performed the previous *hsm* screen. A.W.
827 analyzed the RNAseq and microbiome profiling data. D.T. conducted confocal microscopy
828 imaging. Q.G. performed statistical analysis for the expression of hormone responsive genes
829 and Pearson correlation assays. S.S., Y.L. and L.W. helped with gnotobioc plant assays.
830 Experiments related to *mfec* were performed by R.S. with input from S.Y.H. C.H.H and Y.S.
831 wrote the manuscript with input from all.

832

833 **Competing interests:** Authors declare no competing interests.

834

835 **Code availability**

836 The code related to microbiome sequencing and RNAseq analysis are available on the Haney
837 lab GitHub (https://github.com/haneylab/).

838

839 **Supplementary tables**

840 Table S1. Expression of genes in the shoots and roots of *fer-8* and the parental line by RNAseq.

841 Table S2. Differentially expressed genes in *fer-8* relative to the parental line in shoots and roots.

842 Table S3. Enriched GO terms of highly-expressed genes in the shoots of *fer-8*.

843 Table S4. Expression of different hormone responsive genes.

844

Extended data for

Loss of a plant receptor kinase recruits beneficial rhizosphere-associated *Pseudomonas*

Authors: Yi Song[1,2], Andrew J. Wilson[1], Xue-Cheng Zhang[3,4,5], David Thoms[1,2], Reza Sohrabi[6], Siyu Song[1], Quentin Geissmann[1,2], Yang Liu[1], Lauren Walgren[1], Sheng Yang He[6,7,8] and Cara H. Haney[1,2*]

Affiliations:

[1]Department of Microbiology and Immunology, The University of British Columbia, Vancouver, Canada V6T 1Z3

[2]Michael Smith Laboratories, The University of British Columbia, Vancouver, Canada V6T 1Z4

[3]Department of Molecular Biology, Massachusetts General Hospital, Boston, MA 02114, USA

[4]Department of Genetics, Harvard Medical School, Boston, MA 02115, USA

[5]Current address: DermBiont, Inc, Boston, MA, 02111, USA

[6]Department of Energy Plant Research Laboratory, Michigan State University, East Lansing, MI, USA

[7]Department of Biology, Duke University, Durham, NC, 27708, USA

[8]Howard Hughes Medical Institute, Duke University, Durham, NC, 27708, USA

*Correspondence to: cara.haney@msl.ubc.ca

This PDF file includes: Extended Data Fig. 1-12

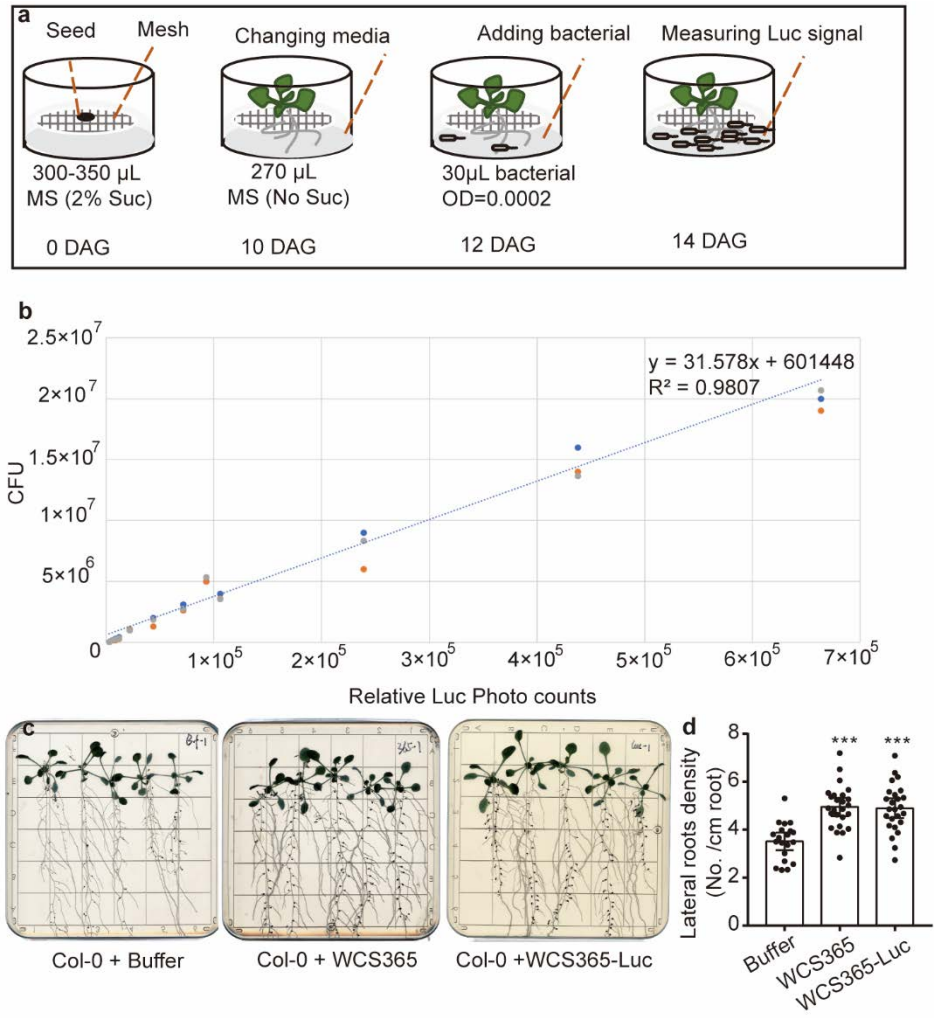

Extended Data Fig. 1. A gnotobiotic plant-rhizosphere microbe interaction system. (a) A diagram showing the 48-well plate based hydroponic plant-rhizosphere commensal interaction system. Seeds were grown on the Teflon mesh which separates shoots and roots after germination. 300-350 µL MS media with 2% sucrose was added to each well. Ten days after germination the media was replaced with 270 µL MS without sucrose. Two days later, 30 µL *P. fluorescens* WCS365-Luc (OD=0.0002) was added to the media, and rhizosphere bacteria levels were quantified after two days incubation using a plate reader. **(b)** WCS365-Luc CFU counts plotted against the relative Luc photo count signal intensities. For different dilutions, 100 µL WCS365-Luc (in 1× MS with 0.1% MES buffer) was transferred to a white opaque 96-well plate for quantifying Luc photo counts. A trend line and R^2 were calculated in excel using the linear trendline option. Different colors of dots represent the three replicates of CFU plating results. **(c)** Insertion of the lux operon into WCS365 did not affect its ability to increase lateral root density. Images show plants treated with buffer, WCS365 or WCS365-Luc. **(d)** Quantification of lateral root density by normalizing to the number of lateral roots per cm of root. n=20, 25 and 25 from left to right. Mean ± SEM is shown, *** $p<0.001$ by Student's t test compared to the buffer treated group.

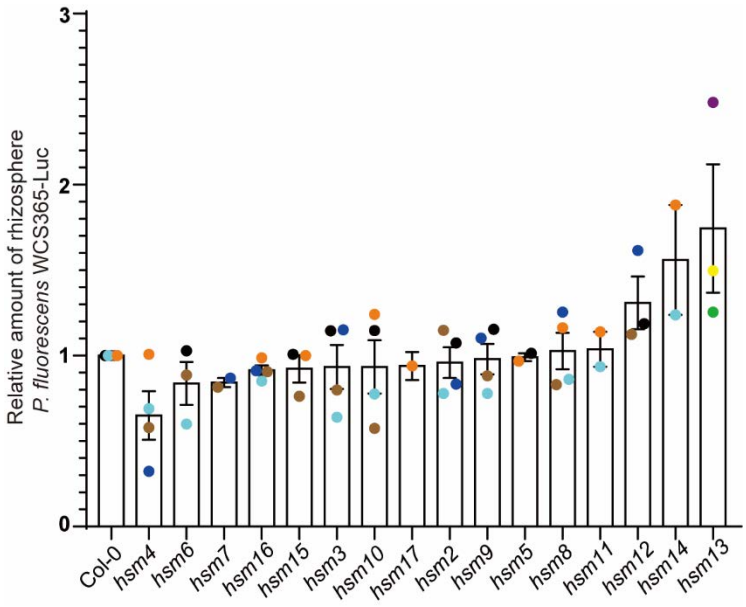

885

886

887 **Extended Data Fig. 2. Relative amount (normalized to Col-0 for each experiment) of *P.***
888 ***fluorescens* WCS365-Luc in the rhizosphere of *hsm* mutants.** Each dot represents the
889 relative fold change of an *hsm* mutant relative to Col-0 from a single experiment; dots of the
890 same color were performed as part of the same experimental replicate.

891

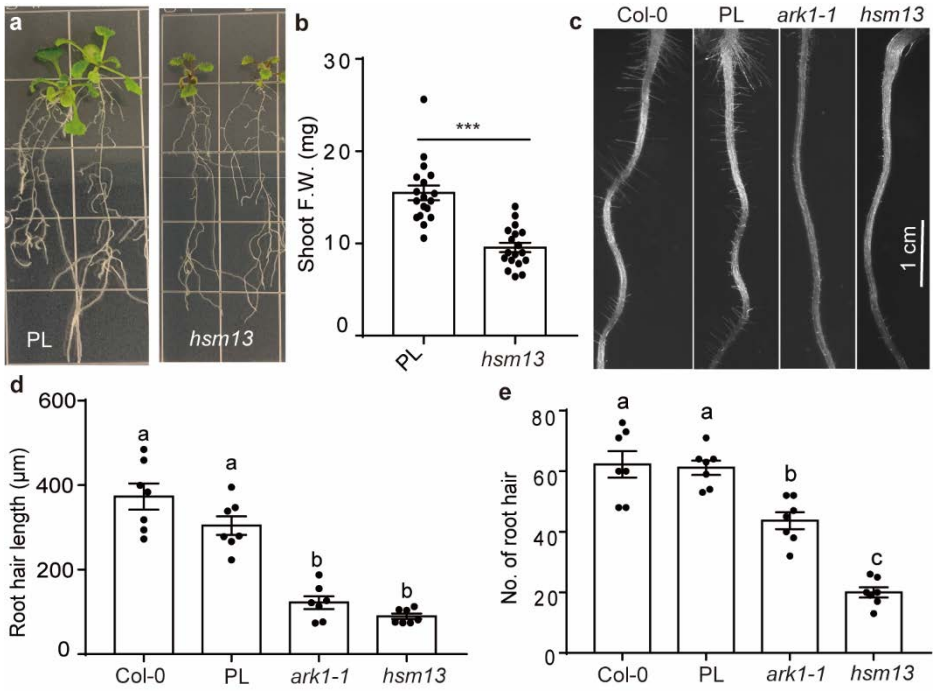

Extended Data Fig. 3. Morphology changes in *hsm13*. (**a-b**) *hsm13* is stunted when grown on axenic plates (½× MS agar) for 15 days. (**b**) Quantification of shoot fresh weight (F.W.) of *hsm13* and the parental line (PL) grown on plates. Student's T-test was used to determine significance, and *** denotes $p < 0.001$. (**c**) *hsm13* shows a root hair developmental defect similar to the previously described *ark1-1* mutant. (**d-e**) Quantification of root hair length (**d**) and number of root hairs (**e**) from 6-day-old seedlings (0.5-4.5 mm region below the root-hypocotyl junction, n=7). Different letters indicate $p < 0.05$ by ANOVA and Turkey's HSD test.

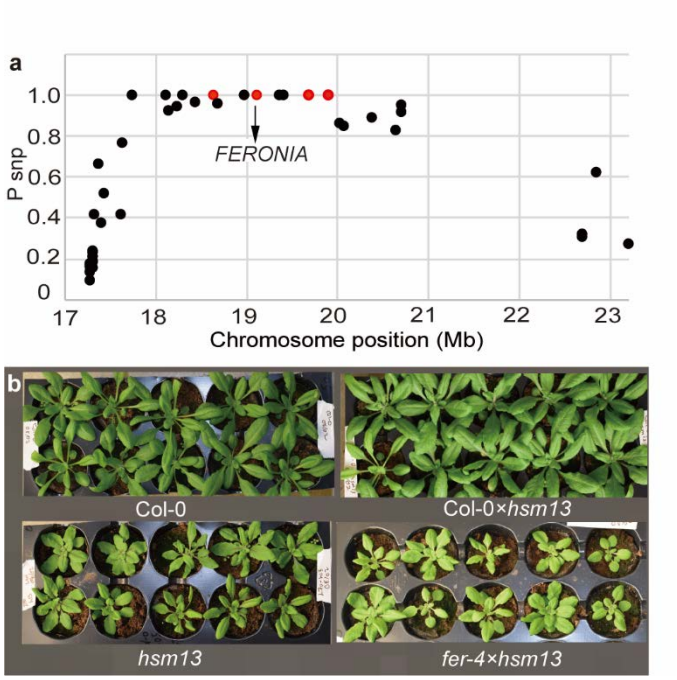

Extended Data Fig. 4. Mapping of *hsm13* based on the stunting phenotype. (**a**) Dot plot of SNP frequency on chromosome 3 in the *hsm13*-like F3s of *hsm13* × Col-0. Red dots represent non-synonymous mutations with P_{SNP}=1 [P_{SNP}=Relative reads abundance of mutant SNP/ (relative reads abundance of mutant SNP+ wildtype SNP)]. **(b)** F1 crosses between *fer-4* × *hsm13* are stunted while Col-0 × *hsm13* F1s had wildtype-like morphology.

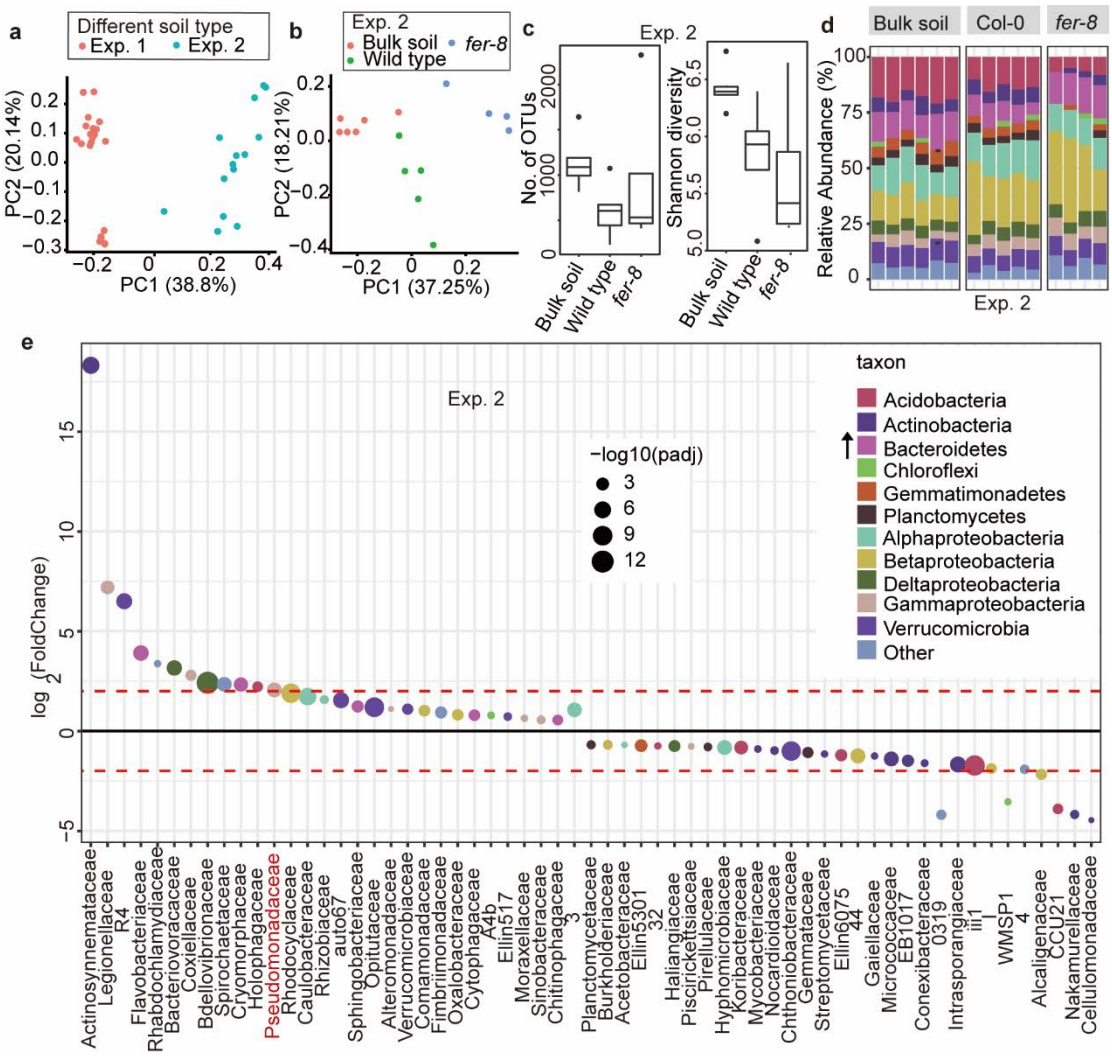

Extended Data Fig. 5. Pseudomonadaceae are robustly enriched in the rhizosphere of *fer-8* grown in soil from experiment 2. (**a**) All samples (bulk soil and plant rhizosphere) are from two independent experiments. Natural soil for Exp. 1 and 2 was harvest from the same site over two consecutive years. (**b**) Principal coordinate analysis (PCoA) shows *fer-8* has a distinct microbiome composition from Col-0 in Exp. 2. (**c**) Alpha diversity indexes in the bulk soil and rhizosphere samples (Exp. 2). (**d**) Relative abundance of bacterial phyla (or Proteobacterial classes) in bulk soil and different rhizosphere samples. The arrow shows the significantly changed taxon in the rhizosphere of *fer-8* relative to the parental line. **(e)** Significantly differentially abundant families between *fer-8* and wildtype rhizosphere. Colors show the taxon information for each family, and the dot size indicates the -$\log_{10}$ transformed adjusted p value; $p<0.1$ was used as a cutoff, red dash line indicates a 4-fold change [$\log_2$(fold change) =2].

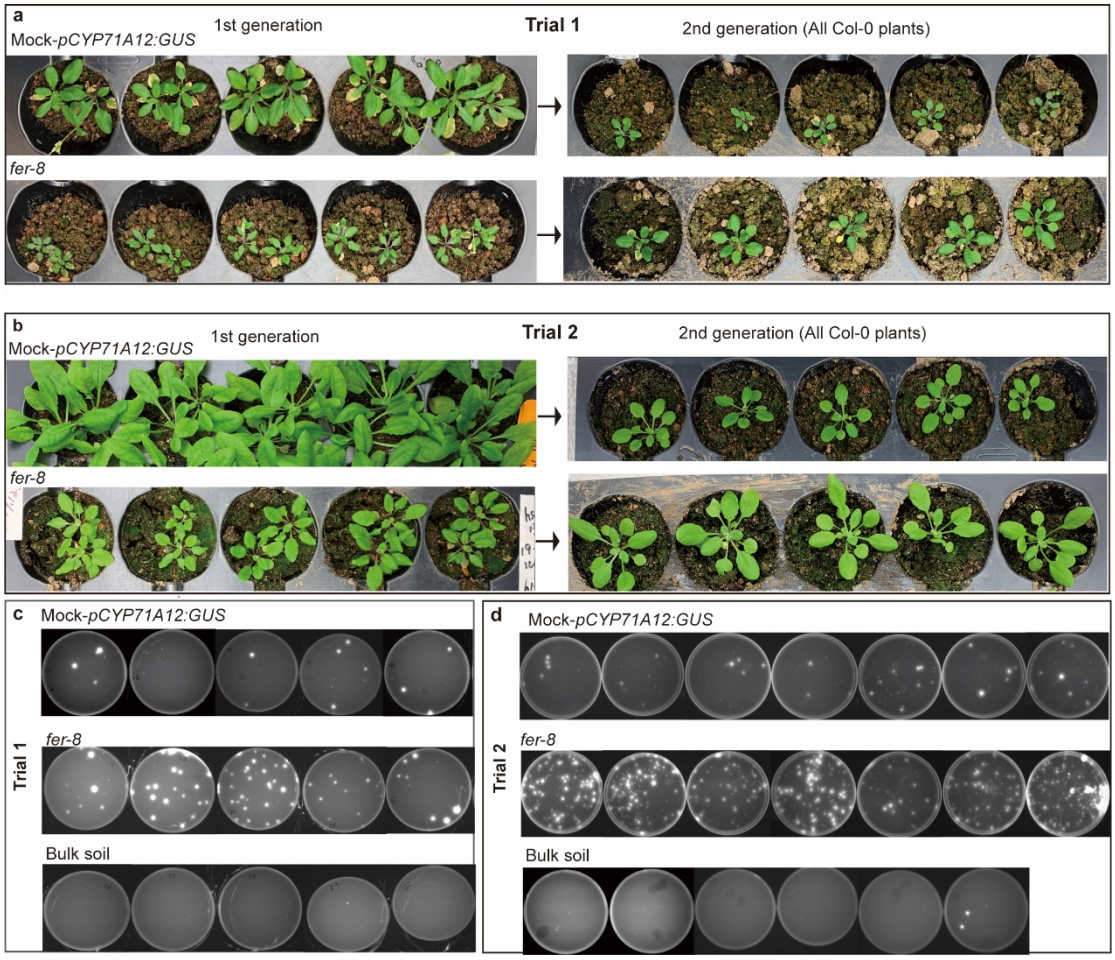

Extended Data Fig. 6. Phenotypes of plants from microbiome transplant experiments. (a-b) Images of 5-week old parental line (PL) and *fer-8* plants grown in natural soil (left panel), and images of 3-week old 2nd generation wildtype plants grown in the soil with previous cultivation of *fer-8* or PL (right panel). **(c-d)** Plating of rhizosphere samples from bulk soil, G1- *fer-8* and G1-PL plants. 100 µl of 0.00025 g/ml serially diluted sample was plated on King's B media and imaged under UV light.

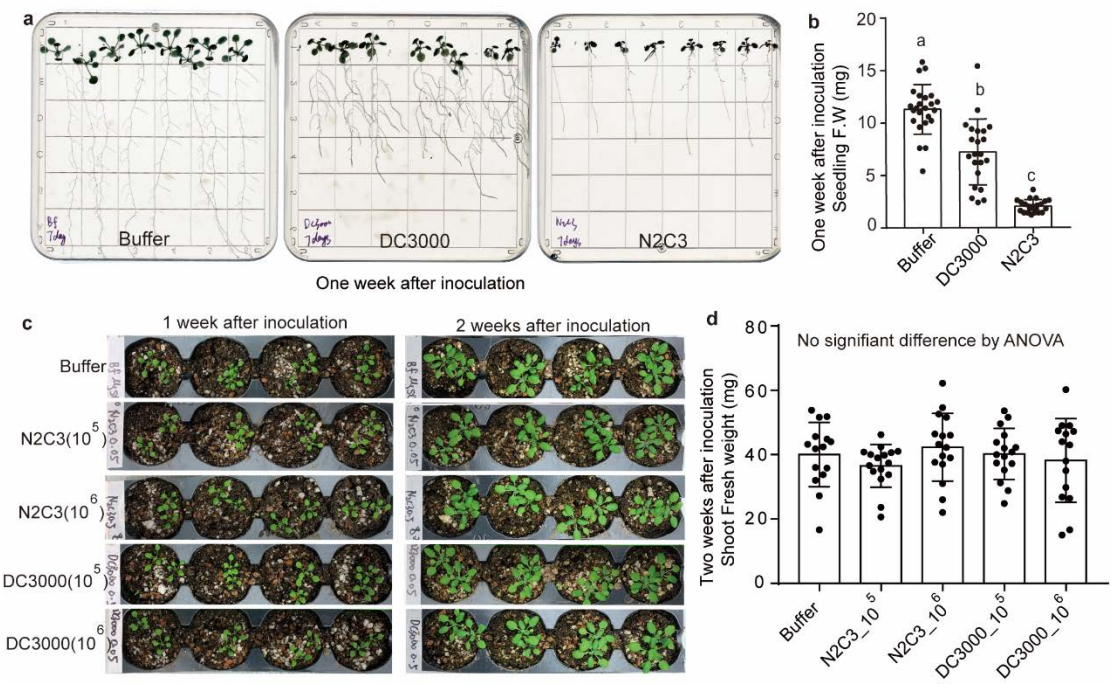

933

934 **Extended Data Fig. 7. *Pseudomonas* pathogens do not efficiently cause disease in soil.** (**a**)
935 Under axenic conditions, *Pst* DC3000 and *Pseudomonas* sp. N2C3 cause stunting one week
936 after inoculation. Seeds were grown on ½× MS without sucrose for 6 days before inoculation.
937 (**b**) Quantification of seedling fresh weight (F.W.) one week after inoculation on plates. (b and
938 d) Mean ± SEM is shown, different letters indicate $p < 0.05$ by ANOVA and Turkey's HSD
939 test. (**c**) Phenotypes of Col-0 grown in natural soil 1 and 2 weeks after rhizosphere inoculation
940 with *Pst* DC3000 or *Pseudomonas* sp. N2C3. For both pathogens, 1 mL OD_{600}=0.5 or 0.05
941 inoculum was added to reach a final concentration of 10^5 or 10^6 CFU/gram soil. (**d**)
942 Quantification of shoot fresh weight 2 weeks after inoculation.

943

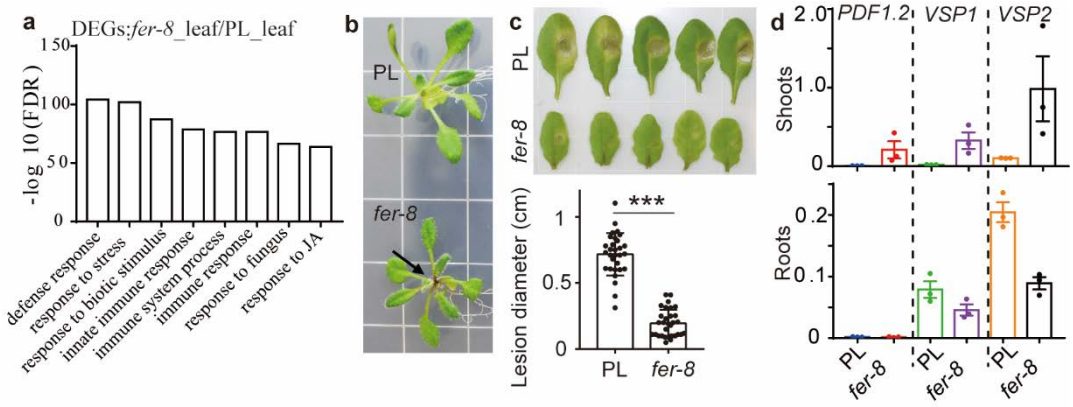

Extended Data Fig. 8. JA signaling is elevated in the shoots of *fer-8*. (**a**) Selected Gene Ontology categories from top 20 significantly enriched GO terms (based on the -log transformed FDR values). GO enrichment analysis was performed with AgriGO. (**b**) Anthocyanin accumulation was observed in the petioles of *fer-8* but not the parental line (PL); representative 2-week old plants grown on plates are shown. (**c**) *fer-8* is resistant to the necrotrophic pathogen *Botrytis cinerea.* The image shows the lesion size 3 days after inoculation. n = 30 and 31 for the PL and *fer-8*, respectively. Data from 2 independent experiments were used for analysis. *** p <0.001 by Student's t-test. (**d**) JA responsive genes were highly expressed in the shoots of *fer-8* but not in the roots. qRT-PCR data from three biological replicates. Gene expression values were normalized to the expression of an internal control gene *EIF4A*. Mean ± SEM is shown.

Extended Data Fig. 9. The effect of the *fer*-8 mutation on hormone signaling is shoot specific and most significantly related to JA signaling. (a-e) The heatmaps show the normalized expression [Z score of TPMs (Transcripts Per Million), Z score = (experimental score – mean)/standard deviation] of hormone-responsive genes in the shoots and roots of *fer-8* and the parental line (PL). JA: Jasmonic acid; ACC: 1-aminocyclopropane-1-carboxylate, an ethylene biosynthetic precursor; BL: brassinolide; IAA: indole-3-acetic acid; ABA: abscisic acid. Each column shows the average values from different replicates within each genotype and tissue. Seedlings were grown under axenic conditions (½× MS-Agar plates). Gene list and expression values for different groups are listed in the Supplementary table S4. **(f-g)** Comparing the rank difference of genes from different hormone responsive pathways and the genome background (non-hormone responsive genes) in shoots and roots. Up, Down and NC means the number of genes with a higher, lower or same ranked in *fer-8* relative to PL, respectively. The p-values were calculated by performing normal bootstrap (5000 replicates) on the mean sign (sign=1, 0 and -1 if a gene is higher, same or lower ranked in *fer-8*) of the rank difference within each pathway (Methods).

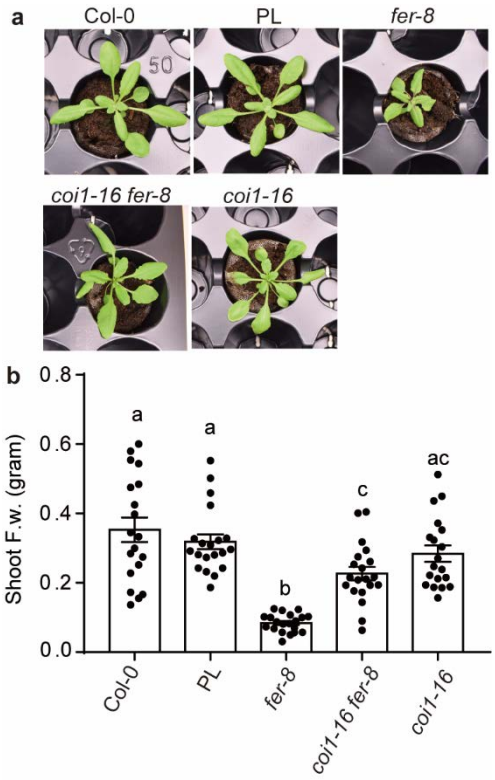

Extended Data Fig. 10. *fer-8 coi1-16* double mutant suppressed the stunting phenotype of *fer-8*. (**a**) Growth phenotypes of Col-0, the parental line (PL), *fer-8*, *coi1-16 fer-8* and *coi1-16*. Images were taken three weeks after germination; (**b**) Quantification of shoot fresh weight (F.w.) of different genotypes at three weeks after germination. Mean ± SEM, different letters indicate $p < 0.05$ by ANOVA and Turkey's HSD test.

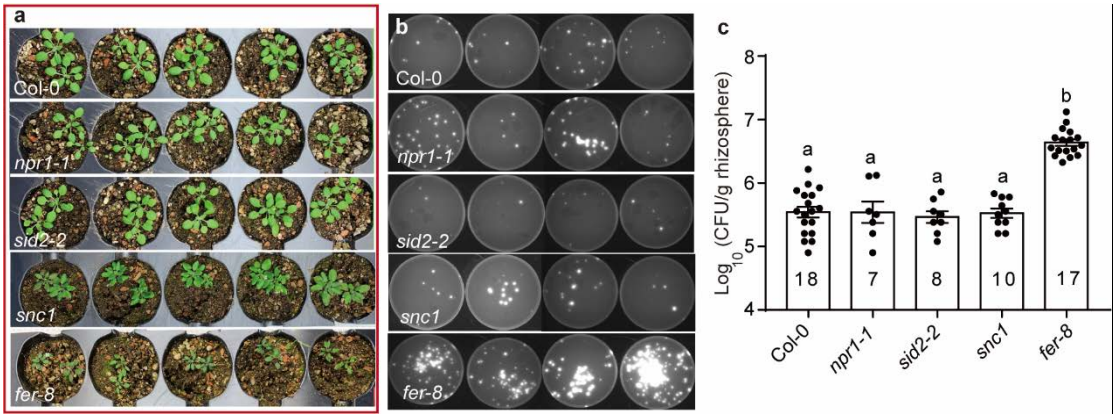

Extended Data Fig. 11. Salicylic acid (SA) mutants do not affect levels of rhizosphere fluorescent Pseudomonads. (**a**) Phenotypes of Col-0, SA signaling and biosynthesis mutants *npr1-1*, *sid2-2*, *snc1*, and *fer-8* grown in natural soil. (**b**) Representative plates of rhizosphere samples from genotypes in (a) are shown. (**c**) Quantification of rhizosphere fluorescent Pseudomonads. Mean ± SEM, different letters indicate $p < 0.05$ by ANOVA and Turkey's HSD test. Numbers represent the biological replicates from 2-4 independent experiments.

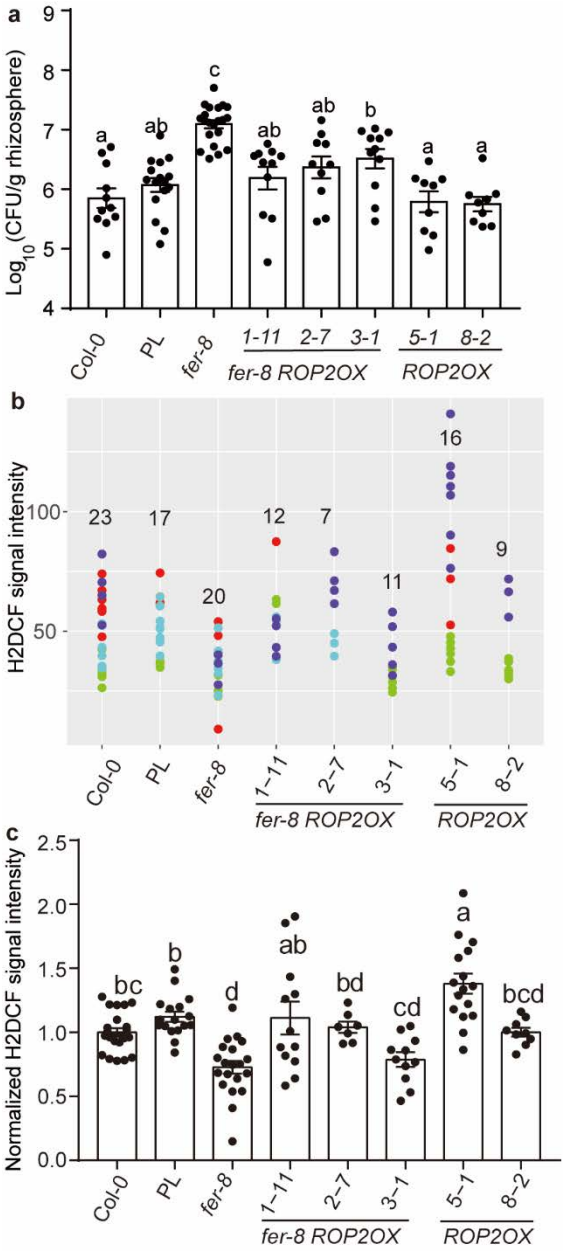

Extended Data Fig. 12. H2DCF staining of ROS levels in roots. (**a**) Overexpression of *ROP2* (a positive regulator of NADPH oxidase) in *fer-8* decreases rhizosphere levels of fluorescent Pseudomonads. n=11, 16, 21, 11, 10, 11, 9 and 9 from left to right (3-5 independent experiments). (**b**) Signal intensity values of root H2DCF staining results from 2-4 independent experiments for Col-0, *fer-8* and *fer-8 ROP2OX* (line 1-11, 5-1 and 3-1), and *ROP2OX (*line8-*2* and 5-1). Numbers on the graph denote the number of measured plants, and dots of the same color were performed as part of the same experimental replicate. (**c**) Data from different independent experiments were normalized to the average values of the Col-0 control from the same experiment. Mean ± SEM, different letters indicate $p < 0.05$ by ANOVA and Turkey's HSD test.